R.D. Apostolova, E.M. Shembel

ON WAYS OF CONVERSION OF SILICON DIOXIDE SIO$_2$ IN LITHIUM BATTERY SYSTEMS: A REVIEW

Ukrainian State University of Chemical Technology, Dnipro, Ukraine

Silicon and silicon oxide compounds SiO, SiO$_2$, SiO$_x$ and SiOC are considered as a promising family of materials for high-energy lithium batteries due to their high theoretical capacity, widespread in nature, low cost, environmental safety and ease of synthesis. Silicon oxide compounds have replaced silicon in the hope of improving the discharge characteristics of lithium batteries. Oxides of silicon show excellent stability during cycling after structure optimization. However, they suffer from the problem of low Coulomb efficiency and high voltage hysteresis (difference in charge and discharge voltage), which prevents their practical application. Significant bulk expansion of silicon oxides during cycling and irreversible loss of capacity in the initial cycles are an obstacle to their large-scale practical use. This review pays attention to the peculiarities of the conversion of SiO$_2$ and its hybrid compounds into the redox reaction with lithium and ways to overcome existing problems. Silicon dioxide is more resistant to bulk expansion than silicon. Various structural formats of nanometer SiO$_2$ have been developed and tested for lithium batteries, such as nanotubes, nanorods, nanowires, nanoparticles, thin films. To solve problems in the SiO$_2$/Li system, a number of SiO$_2$ composites with carbon, graphene, active and inactive metals, etc. have also been proposed and studied. Analyzing the results of the studies, we found a significant role of the solid electrolyte interphase film in the efficient conversion of SiO$_2$. In turn, the formation of a film on silicon dioxide depends on the method of synthesis of dioxide, which introduces impurities into the final synthesis product. Impurities contribute to the distortion of the solid electrolyte interphase film during the cycling of the SiO$_2$/Li system, and the loss of discharge capacity. SiO$_2$ dioxide obtained in a dry environment of a ball mill differs favorably from that obtained from solutions. Many efforts have been made to overcome the problems in Si-containing electrode materials, however, they have to go a certain way for large-scale practical application.

Keywords: silicon oxide, silicon, lithium-ion battery, electrochemical transformation pathway, degradation process, composite compound, problem-solving strategy.

Ways of conversion of silicon dioxide SiO$_2$

In early studies, it was believed that SiO$_2$ dioxide was electrochemically inactive against Li [1,2]. In fact, it was considered as an inert matrix-buffer, which resists the bulk expansion of the active components during lithiation/delithiation, and that the reduction of SiO$_2$ to Si and Li$_2$O by reaction (1) was thermodynamically impossible [2]:

$$SiO_2 + 4Li^+ + 4e^- \rightarrow Si + 2Li_2O, \quad E^0 = 0.69 \text{ V} \quad (1)$$

When silica interacts with lithium, silicon is formed [3], the transformation of which in the processes of lithiation in Si and SiO$_2$ is described in detail in reviews [4,5]. High-lithium amorphous silicon suddenly crystallizes when it reaches a potential of 50 mV vs. Li$^+$/Li electrode, forming a lithium-silicon phase, identified as Li$_{15}$Si$_4$. Delithiation of the Li$_{15}$Si$_4$ phase leads to the formation of amorphous silicon. Silicon anodes in cycling above 50 mV avoid the formation of the phases, which improves cyclicity.

The mechanism of the reaction between SiO_2 and Li is not fully understood, and there are still disputes about the reaction pathways and end products. This review complements the information on the interaction of SiO_2 with lithium, provided earlier [5]. Theoretical calculations and in situ studies were used to identify the mechanism of SiO_2 lithiation [6−9]. When using the theory of functional density (DFT) and molecular dynamics (MD), it was found that the formation of Li_2O and Si−Si bonds (complete reduction) is energy disadvantageous, and only two Li attack and break the Si−O bond [6].

In studies of the SiC composite(core)@SiO_2(shell), the SiC nucleus was inactive with respect to Li, while the shell showed signs of activity [7].

According to the theoretical calculations by Balbuena et al., Li is included in SiO_2 due to the rupture of the Si−O bond and due to the partial reduction of Si atoms [8]. The breakdown of the Si−O bond becomes less advantageous at high lithium levels, with the formation of the Si−Si bond and the emergence of Li_6O complexes. According to ref. [10], the most advantageous energy formation of $Li_2Si_2O_5$ for lithiation SiO_2 is shown.

Direct experimental confirmation of electrochemical reduction of SiO_2 using nuclear magnetic resonance (NMR), X-ray photoelectron spectroscopy (XPS), high-resolution transmission electron microscopy (HRTEM) and Energy dispersive X-ray analysis (SAED) [11] was obtained. It was found that at the early stage of silica lithiation oxide Li_2O is formed. In the subsequent lithiation, a mixture of Li_4SiO_4 and Li_2O is formed. Guo and colleagues proposed a mechanism, according to their XPS data [11]:

$$SiO_2 + 4Li^+ + 4e^- \rightarrow 2Li_2O + Si, \qquad (1)$$

$$SiO_2 + 4Li^+ + 4e^- \rightarrow Li_4SiO_4 + Si, \qquad (2)$$

$$Si + xLi^+ + xe^- \rightarrow Li_xSi. \qquad (3)$$
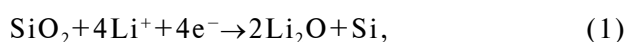
Fultz et al. consider the reduction of SiO_2 oxide thermodynamically possible process [12].

A promising material for the creation of electrochemical current sources based on it is nanodispersed silicon dioxide, which is obtained from silicon halides by the so-called pyrogenic method. Mironjuk et al. [13] tested nanodispersed pyrogenically obtained silica as a material for the positive electrodes of a lithium current source. The energy capacity of the elements depends on the average diameter of the primary SiO_2 particles and the degree of their aggregation. The use of nanodispersed silica with an average particle diameter of 9 nm is considered promising. When discharging a lithium cell with a cathode based on pyrogenic dioxide silicon in the galvanostatic mode (current density was 6.5 $mA \cdot g^{-1}$), the specific capacity and energy of the active material reaches 1865 $A \cdot h \cdot kg^{-1}$ and 4837 $W \cdot h \cdot kg^{-1}$, respectively. The obtained results testify to the prospects of pyrogenic silica for its use as a material of positive electrodes of lithium power sources.

To obtain high-performance anode materials for lithium-ion batteries, innovative and practical concepts have been proposed that use easy amorphization of quartz powders by mechanical grinding in high-energy ball mills [14]. Metal Si and amorphous silicon dioxide, as well as gaseous oxygen were isolated from very stable crystalline silicon dioxide during grinding. Silicon crystals with a size of 5 nm were dispersed in a matrix of amorphous silicon dioxide. The crushed material reacts with Li, demonstrating excellent electrochemical characteristics with a capacity of 800 $mA \cdot h \cdot g^{-1}$ for 100 cycles. In the reaction with Li electrodes were used, which include 70% crushed SiO_2, 15% carbon black Ketchen, 15% polyamidimide, in a composition with N-methylpyrrolidone. The electrodes were dried under vacuum at 200^0C for 4 hours.

Analyses showed that Si and $Li_2Si_2O_5$ phases were observed when the electrode potential was reduced to 0.27 V vs. Li^+/Li. At 0.24 V, lithium silicate Li_4SiO_4 was also formed. At the potential of 0.01 V, phase $Li_{15}Si_4$ was observed. Among these Li-silicates, the reversibility of the $Li_2Si_2O_5$ phase was noted, while the Li_4SiO_4 phase formed during the synthesis of the SiO_x/C composite was irreversible. Reactions of SiO_2 with Li during the 1st cycle are given as follows:

Inclusion Li^+

0.27 V: $a\text{-}SiO_2 + (4/5)Li^+ + (4/5)e^- \rightarrow \rightarrow (2/5)Li_2Si_2O_5 + (1/5)Si, \qquad (4)$

0.24 V: $a\text{-}SiO_2 + 2Li^+ + 2e^- \rightarrow (1/2)Li_4SiO_4 + (1/2)Si, \quad (5)$

0.0 V: $Si + (15/4)Li^+ + (15/4)e^- \rightarrow (1/4)Li_{15}Si_4, \qquad (6)$

Extraction Li^+

0.34 V: $Li_{15}Si_4 \rightarrow 15Li^+ + 4Si + 15e^-, \qquad (7)$

0.39 V: $Li_2Si_2O_5 + (1/2)Si \rightarrow (5/2)SiO_2 + 2Li^+ + 2e^-. \quad (8)$
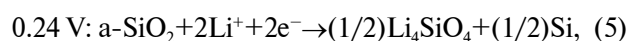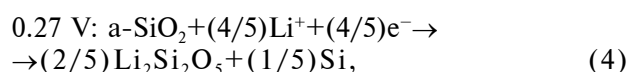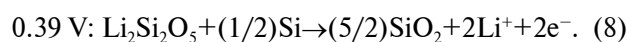
Si appears as a result of reactions (1) and (2), as well as grinding. In the 10th cycle, reversible phases,

such as $Li_{15}Si_4$ and $Li_2Si_2O_5$, were repeatedly formed. Crystal structures $Li_2Si_2O_5$ (SG Ccc2, a=5.807 Å, b=¼14.582 Å, c=¼4.773 Å) and Li_4SiO_4 (SG P121/M1, a=5.147 Å, b=¼6.094 Å, c=¼5.293 Å), as can be seen from their parameters, differ. The length along the b-axis of the orthorhombic $Li_2Si_2O_5$ unit cell is 2.4 times greater (14.582 Å) than that of monoclinic Li_4SiO_4 (6.094 Å). The open tunnel structure along the c axis in the $Li_2Si_2O_5$ phase can provide easy diffusion paths for Li ions and the reversibility of the $Li_2Si_2O_5$ phase. In the case of the 24-hour grinding sample, the sharp decrease in charge capacity compared to the discharge capacity during the 1st cycle was due to the formation of irreversible lithium silicate (Li_4SiO_4). Although 24-hour ground SiO_2 showed a low initial Coulomb efficiency (37%), it was reduced to 99% in the next cycle. In addition, the preservation of the electrode capacity was 90% on the 100th cycle and more than 80% over 200 cycles. To increase the initial Coulomb efficiency, it was proposed to adjust the voltage to 0.27 V to form the reversible phase of $Li_2Si_2O_5$ in the 1st cycle.

Bulk SiO_2 shows low electrochemical activity against Li due to sluggish diffusion of Li^+ and low intrinsic electrical conductivity. Reducing the particle size increases the electrochemical activity of SiO_2 [15−18].

Three-dimensional aerogels made of graphene doped with nitrogen with different loading masses SiO_2 (SiO_2/NGA) were synthesized by light hydrothermal means [17]. This composite structure has significantly increased capacity due to surface and interface design, and the ability to significantly absorb bulk expansion of silica. When used as an anode material for lithium-ion batteries, the SiO_2/NGA nanocomposite can provide a specific capacity of more than 1000 mA·h·g^{-1} at a current density of 100 mA·g^{-1} with long cycling stability and demonstrate typical pseudo-capacity. The creation of a composite of nitrogen-doped aerogel is an effective way to improve Si-based electrodes for LIB.

In the Li_2O-SiO_2 system, Li_2SiO_3 and Li_4SiO_4 compounds are formed due to solid reactions with lithium [19]. The initial specific capacitance of Li_2SiO_3 and Li_4SiO_4 reaches 136 and 129 mA·h·g^{-1}, respectively. Increased productivity of the redox reaction with lithium is manifested after the application of carbon coating. The initial specific discharge capacity of Li_2SiO_3 and Li_4SiO_4 with carbon coating can reach 230 and 220 mA·h·g^{-1}, respectively. The oxide film on the surface of the silicon electrode has different effects on its electrochemical conversion to the redox reaction with lithium depending on the method of oxidation of silicon [20]. In the case of

the Si−1 sample obtained from the H_2O_2/H_2SO_4 solution, a thin, very dense SiO_x film was obtained. In the second case, the Si−2 oxide layer was porous and thick. It was obtained by dissolving the virgin oxide layer on silicon in HF solution. SEM images showed that both modified samples contained nanoparticles with an average diameter of 100 nm. The obtained powders were mixed with conductive carbon XC-72 (Cabot, Boston, MA, USA) and 4% aqueous solution of carboxymethylcellulose (CMC) in a weight ratio of 6.0:2.5:1.5. During the 1st scan in cyclic voltammetry, the Si−1 sample in the cathode part contains a small peak at 1.8 V vs. the Li^+/Li electrode associated with partial reduction of the surface oxide, and also contains a sharp peak starting from 0.2 V vs. Li^+/Li, associated with a two-phase silicon lithiation process. In the oxide scan of the Si−1 sample, the two peaks at 0.45 and 0.55 V correspond to the delicacy reactions of the Li_xSi alloy formation, which continue through the intermediate phase of $Li_{12}Si_7$. During the first potential scan, the Si−2 sample revealed two peaks associated with the reduction of silicon oxide at 1.80 and 1.05 V. The kinetics of Li_7Si_{12} formation for the Si−2 sample is shown. Because this reaction involves the removal of bulk silicon (core), it must be independent of the chemistry of the oxide surface. Galvanostatic cyclicity of the modified materials showed significant differences in the characteristics of Si−1 and Si−2. The retention capacity of the modified sample (Si−1) reached 83% after 50 cycles, compared with 99.3% for Si−2. The significant difference in the preservation of capacity between the two materials is due to the influence of different characteristics of the oxide surface.

The use of silicon in LIA is complicated, among other factors, by insufficiently stable solid electrolyte interphase (SEI). The formation of SEI depends on the surface of Si, which is covered with oxide (SiO_x). In the study [21], three different Si surfaces were compared using Si plates coated with natural SiO_x 1.3 nm thick, thermally grown SiO_2 1.4 nm thick, and samples without SiO_x. The latest samples showed the worst electrochemical parameters with CE of about 94%, with the thickest SEI film and the highest polarization during lithiation. Oxide coated surfaces achieved significantly better results, showing CE above 99% after the second cycle, low polarization during lithiation and a thinner and more stable SEI film. Oxides reduce the potential for electrolyte decomposition, and promote the formation of SEIs with fewer P−F species. However, it was found that the CE in the case of the surface with natural oxide decreases from the fifth cycle and correlates with

electrolyte reduction. 1−2 nm thick thermal coating is optimal to achieve a stable SEI that minimizes side effects and maintains efficient cycling.

It was found [22] that the SiO_2 layer on silicon particles, a promising electrode material for future generation of lithium-ion batteries, can adversely affect the conversion of silicon electrode, slow the transport of lithium ions at the SiO_2/Si interface, lead to low reverse capacity and increasing the impedance of charge transfer. When a low potential is applied to the Si electrode, the oxide layer can quickly turn into a silicate form in the range of 0.01−1.00 V vs. Li^+/Li. This leads to irreversible consumption of lithium ions with a cardinal loss of capacity in the lithium−ion system.

Despite a huge number of studies of electrochemical-mechanical behavior of energy-saving materials, the mechanical behavior of amorphous SiO_2 during the electrochemical reaction remains largely unknown. The evolution of stresses, electronic structure, and mechanical deformation of SiO_2 were systematically investigated by calculating the first principles and finite element method [23]. The structural and thermodynamic role of O in the amorphous Li−O−Si system is described. The Si−O bonds in SiO_2 show high mechanical strength, but are mechanically softened by the introduction of Li-rich phase SiO_2. The finite element model, including the kinetic model for anisotropic expansion, demonstrates the long-term cyclic stability of Si−SiO_2 core-shell nanoparticles. It is mainly due to the reaction kinetics and high mechanical strength of SiO_2. These results give a fundamental idea of the chemo-mechanical behavior of SiO_2 for practical use.

A method for the synthesis of a thin-layer composite SiO_2/Ni electrode is proposed, in which amorphous nanometer silicon dioxide obtained by the method of sulfuric acid deposition is enclosed in a nickel matrix for efficient use in negative electrodes of lithium-ion film battery [24]. The synthesized SiO_2 was used for galvanic production of a thin-layer SiO_2/Ni composite on the cathode of nickel foil with a nickel anode. The cathode was placed horizontally and a suspension of SiO_2 in the electrolyte for nickel plating with thorough stirring was poured into the cell. After 5−20 minutes, during which SiO_2 particles sedimented on a nickel base, the current was turned on for a specified time. The composition of the electrolyte for the deposition of the composite was as follows, g·L^{-1}: $NiSO_4$·$7H_2O$ 150; Na_2SO_4·$5H_2O$ 25; H_3BO_3 15; KCl 10; SiO_2 2; pH 5−6. The electrolysis conditions were as follows: $S_{cathode}$:S_{anode}=1:20; $i_{cathode}$=1.5−2.0 mA·cm^{-2}. Heat treatment was conducted at 105^0C for 6−7 h. The

size of the synthesized particles is mostly 12−16 nm and does not exceed 22 nm.

Discharge-charging curves of the synthesized electrode in the model Li-battery in dimensions CR2016 with electrolyte dimethoxyethane (DME, Merck), dioxolane (DOL, Acros), 1 mol·L^{-1} $LiBF_4$ depend on the duration of sedimentation of silica on the Ni-base, which determines its mass in the sediment. At duration of 5 minutes, the starting discharge curve changes monotonically within the voltage of 1.20−0.05 V. At duration of 15−20 minutes, the discharge curve consists of two sections: horizontally inclined within 1.4−1.2 V and purely horizontal within 0.25−0.35 V at the current density of 20−100 mA·cm^{-2} (Fig. 1). In the subsequent cycles the inclined site disappears, horizontal anode and cathode sites remain (Fig. 2).

The obtained results show the homogeneous distribution of SiO_2 dioxide in the matrix, which provides accessible transport of charged particles within the nickel matrix and contributes to the horizontal orientation of discharge-charging (E vs. Q) curves of SiO_2/Ni electrode, as well as cycling stability in the voltage range 0.40−0.10 V at low density of discharge and charging currents.
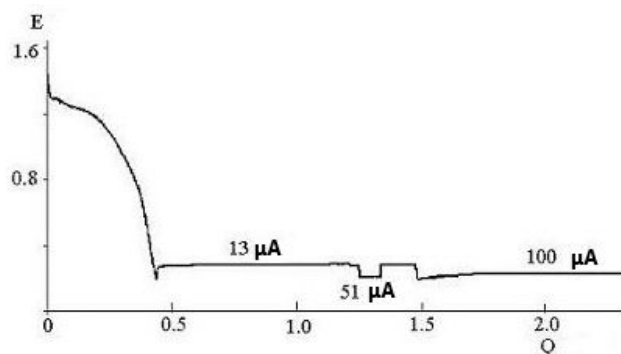
Fig. 1. Changing the profile of the discharge curve SiO_2/Ni with a change in current density
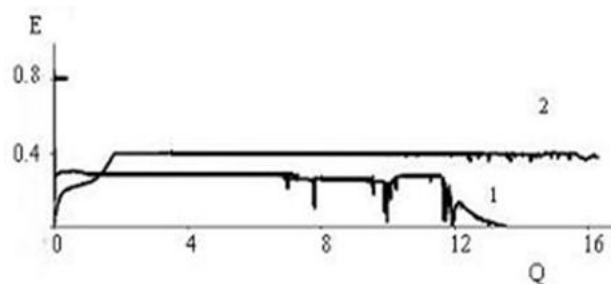
Fig. 2. Discharge-charging curves of the SiO_2/Ni composite with increasing degree of charge/discharge of the SiO_2/Ni composite in the 10th cycle: $i_{discharge}$=i_{charge}=0.05 mA·cm^{-2}. 1 − discharge, 2 − charge

Outside the specified range, with increasing charging current density and discharge, at a discharge voltage below 0.07−0.05 V, degradation electrode processes associated with bulk expansion of silicon dioxide are observed. Their appearance is evidenced by fluctuations in the curves (Fig. 2).

It is known that in the electrodes based on silicon and its oxides, the dimensional changes in the horizontal and vertical directions that occur during cycling in a lithium battery differ from each other. There is a mechanical tension in them. The formation of new phases during the cycling of Si-containing electrodes also contributes to the development of inhomogeneous bulk changes. There is a rupture of the electron-ion transport path, an increase in the internal resistance of the electrode, as well as the rupture of the surface protective solid-electrolyte film SEI on silicon oxide. Dense stable film, which prevents side effects that lead to lithium consumption, continuously updated during rupture, becomes unstable. Mechanical stress leads to the destruction of particles, grinding of the material, loss of contact between its particles, violation of the integrity of the electrode, the fall of the discharge capacity. As a result of fragmentation of the electrode in delithiation, which leads to an increase in its internal resistance, the discharge curve decreases, approaching the deposition potential of lithium, after which lithium cycling (deposition-dissolution) takes place. A similar interaction of base oxides (stainless steel) with lithium is shown in studies of a thin-layer $LiCoO_2$ electrode in a model lithium battery [25].

The role of the active SiO_2 material becomes predominant with increasing the degree of filling of the nickel base in the investigated composite electrode, which is observed with increasing sedimentation time of silicon dioxide. Then the electrochemical activity of the thin-layer SiO_2 electrode is manifested in a narrow voltage range: between 0.40−0.10 V. In this case, it is possible to achieve high bit capacitance characteristics comparable to those defined with a silicon electrode [26] which was received by a technically complicated method of photoelectric chemical etching of the washers of monocrystalline n-silicon. For long-term stable cycling of a SiO_2/Ni electrode with high Coulomb efficiency, it is important to clearly limit the operating range of the cycling voltage, avoiding the formation of phases associated with significant bulk expansion. This is easy to do, taking advantage of the discharge-charging curves of the studied composite − the constancy of the operating voltage over a long period in the processes of charge and discharge.

Amorphous films of silicon dioxide occur on the surface of silicon naturally under the influence of the atmosphere. When using silicon in the electrodes of lithium-ion batteries, the characteristics of its surface lithium are important for understanding the operation of Si-anodes. Analysis of the theory of the functional density of lithiation of amorphous lithium silica reveals the mechanisms of lithiation and the role of surface functional groups in lithiation reactions and the film structure [8]. The surface concentrations of silanol groups and the structure of the optimized model of the amorphous hydroxylated silicon dioxide film are consistent with those observed experimentally. It has been established that lithium is included in SiO_2 by breaking the Si−O bonds and partially reducing the Si atoms.

Features of the interaction of various modifications SiO_2 with lithium

Mechanisms of interaction of SiO_2 with lithium in thin films

Lithiation of SiO_2 thin films obtained by reactive radiofrequency sputtering was first studied in the work [27]. Films with a thickness of 400 nm had a load of SiO_2 of 0.11 mg·cm^{-2}. Cyclic voltammograms at a scan sweep rate of 0.1 V·s^{-1} were obtained in the electrolyte $LiPF_6$ 1 mol·L^{-1}, ethylene carbonate: dimethyl carbonate (1:1 volume, Merk). The reverse discharge capacity of SiO_2/Li, which varies cyclically between 0.01 and 3.00 V in the galvanostatic process, is in the range from 416 to 510 mA·h·g^{-1} during the first 100 cycles. The capacity decreases during the first 100 cycles by 13.7%, its drop of less than 0.01% per cycle indicates electrochemically active SiO_2 nanostructured material. The authors believe that the plateau with a high voltage of about 1.50 and 0.82 V should be a feature of the electrochemical reaction of SiO_2 with lithium.

Three cathode peaks at 1.20; 0.77 and 0.01 V at the initial discharge and two anode peaks at 1.57 and 1.75 V are observed on voltammograms. In subsequent cycles, the cathode peaks at 1.20 and 0.77 V go to 1.54 and 0.87 V, respectively. The two anode peaks appear at 1.60 and 1.87 V after the initial cycle. It was found that initially the structure of silicon dioxide belongs to the spatial group (P63-mmc). When SiO_2 is discharged to 0.1 V, $Li_2Si_2O_5$ (spatial group Ccc2) is formed; when it is charged to 3.0 V SiO_2 (spatial group P6222) is formed. According to photoelectron spectroscopy, the concentration ratio of Si/O in silicon dioxide is 1.00/1.97.

Ex-situ data HR-TEM, SAED and XPS support the inverse reaction of SiO_2 to $Li_2Si_2O_5$ conversion.

The mechanism of electrochemical reaction of SiO_2 with lithium was expressed by the authors as reactions (3) and (9).

$$5SiO_2 + 4Li^+ + 4e^- \rightarrow 2Li_2Si_2O_5 + Si \qquad (9)$$

In reaction (9), the theoretical discharge capacity of SiO_2 reaches 357.3 mA·h·g^{-1}. It was found that this value is less than the inverse capacity of the discharge of 465 mA·h·g^{-1} according to the curve of discharge/charge. Therefore, another contribution to the inverse capacity may come from the fusion of Si with Li by reaction (3). The formed alloy cannot be seen using SAED due to the formation of metastable phases and amorphization [28]. Discharge plateaus below 0.4 V in the discharge/charge curve and cathode peak at 0.01 V in CV data are attributed to the Li-Si fusion process. Two redox pairs 1.0−1.75 V and 0.77−1.57 V in the first cycle were attributed by the authors to the interaction of SiO_2 with lithium to obtain $Li_2Si_2O_5$ and Si. Electrochemical features of nanostructured SiO_2 thin film differ from those of SiO_x film (x<1.1), when the process of reversible discharge on the plateau below 0.4 V is predominant [29], and Li_2O and Li-silicates are formed during discharge [30].

Peculiarities of electrochemical transformation of SiO_2-nanotubes with lithium

A number of architectural formats based on SiO_2 have been fabricated and characterized as anodes, which include nanocubes, thin films and nanoparticles with carbon coating, nanospheres, etc. [31−33].

In the study [34], SiO_2NT nanotubes were fabricated using a two-step solid growth method and evaluated as an anode for lithium-ion batteries. The amorphous SiO_2 layer was deposited on AAO commercial templates by a vapor-phase process and thermal degradation of polydimethylsiloxane, a non-toxic and environmentally friendly organosilicon. Electrochemical parameters of the interaction of SiO_2NT with lithium were characterized in an electrolyte containing 1 M LiPF$_6$ in (EC:DEC=1:1, vol./vol.). The electrodes were prepared by mixing SiO_2NT powder, acetylene carbon black, Super P and fluoro-polyvinylidene (PVdF) in a weight ratio of 5:3:2. The suspension was pressed onto copper foil and allowed to dry at 90⁰C for 12 hours. The loading density of SiO_2NT on the copper foil was 2.73 mg·cm^{-2}.

SiO_2 nanotubes show a very stable reversible capacity of 1266 mA·h·g^{-1} after 100 cycles with slight attenuation of the tank. SiO_2 NT anodes experience an increase in capacitance during the first 80 cycles due to the increase in the Si phase during SiO_2 reduction. The hollow morphology of SiO_2 nanotubes provides a large expansion of the volume experienced by Si-based anodes during soldering, and helps to preserve the interfacial layer of the solid electrolyte. The thin walls of SiO_2 nanotubes can effectively reduce the distance of the diffusion path of Li-ion and, thus, provide a favorable cycling rate. The high aspect ratio of these nanotubes allows the use of a relatively scalable method of manufacturing nanosized anodes based on SiO_2.

High performance is also achieved with silica in the format of composite microspheres. In the study [35], silica/graphite anode material was synthesized in situ by hydrolysis-calcination using ethyl orthosilicate as a source of silicon. The results of the study by the methods of galvanostatic charge-discharge, cyclic voltammetry and electrochemical impedance spectroscopy showed that amorphous silica microspheres were embedded in the graphite matrix. This structure not only strengthened the Si−O−C bond, but also improved the composition of the solid electrolyte interphase. The specific capacity of the silica/graphite anode can be stabilized at about 450 mA·h·g^{-1} after 300 cycles at a current density of 100 mA·g^{-1}, which leads to stable storage of lithium due to the synergistic effect between silica and graphite.

Porous SiO_2 nanoparticles as a promising material for negative electrodes LIB

When used as electrode materials for LIB, hollow porous nanoparticles can reduce the diffusion path length of lithium ions with improved cyclicity and reduce structural deformation and volume fluctuations when the electrode material interacts with lithium. The preparation of hollow porous SiO_2 nanocubes in a two-step method with a rigid template and their potential use as anode materials for LIB was reported in ref. [36]. The procedure for obtaining SiO_2 nanocubes is as follows: nanoparticles $Co_3[Co(CN)_6]_2$, which are used as a template, are coated with silicon dioxide and sintered at 550⁰C for 1 hour. First, $SiO_2@Co_3O_4$ nanocubes are obtained, and after their acid etching, SiO_2 nanocubes are obtained.

Two peaks in the first cycle in the reduction process, 1.3 V and 0.55 V, are observed on the cyclic voltammograms of SiO_2 nanocube electrodes. They are attributed to the processes of electrolyte decomposition and film formation (SEI). The SEI film is formed in the first cycle, followed by stable efficient cycling. The discharge and charging capacities of the 1st cycle are 3084 and 1457 mA·h·g^{-1}, respectively, with a low initial Coulomb efficiency

of 47% CE. The discharge capacity of the 2nd cycle is equal to 1807 mA·h·g^{-1}. Such a large irreversible capacity (1277 mA·h·g^{-1}) can be attributed to the formation of the SEI layer and electrochemical reactions between lithium ions and SiO_2 [37].

According to HRTEM and SAED, the mechanism is presented as reversible reactions (3) and (9). It is concluded that three types of reactions exist between silicon dioxide and lithium. The mechanism of reaction with the production of Li_2O and Si shows the highest reversible capacity of 1961 mA·h·g^{-1}.

SiO_2 nanowires when interacting with lithium in LIA

SiO_2 nanowires were prepared for negative electrodes of lithium-ion batteries by the sol-gel process using a template [38]. The amorphousness of SiO_2 was confirmed by X-ray diffraction and Fourier transform infrared spectroscopy. The results of scanning electron microscopy and transmission electron microscopy show that the SiO_2 nanowire has a diameter of about 100 nm and a length of about 30 mm. The results of cyclic voltammetry and galvanostatic research were performed in the potential range of 0.05−3.00 V. At a current density of 200 mA·g^{-1}, specific capacity of the first cycle reaches 2252.6 mA·h·g^{-1} with CE 60.7%. Even after about 400 cycles, 97.5% of the initial specific capacity was still maintained. Moreover, when the current density was increased to 2500 mA·g^{-1}, high specific capacity was found. Data of cyclic voltammetry and galvanostatic research give the basis for detection of the mechanism of electrode transformation. In the first cycle, there are two obvious recovery peaks located at 1.5 V and 1.0 V. The peak at 1.5 V facilitates the decomposition of the electrolyte solution and the formation of a solid electrolyte layer (SEI) on the anode surface, which is an important cause of irreversible initial discharge. Peak at 1.0 V indicates side effects. When the material was first discharged, amorphous SiO_2 was reduced to Si to form $Li_2Si_2O_5$ or Li_4SiO_4 [37]. The irreversible phase of Li_4SiO_4, formed as a result of reaction (2), consumes a large amount of Li^+, which is another significant part of the irreversible capacity. The authors summarized the bit processes as the reactions (2), (9) and (10).

$$4Si+15Li^++15e^-\leftrightarrow Li_{15}Si_4 \qquad (10)$$

Charging processes involve reactions (3), (11) and (12).

$$Li_{15}Si_4\leftrightarrow 4Si+15Li^++15e^- \qquad (11)$$

$$2Li_2Si_2O_5+Si\leftrightarrow 5SiO_2+4Li^++4e^- \qquad (12)$$
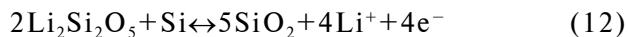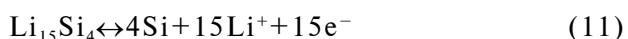
The profile of the silica composite with nanowires repeats the profile of the theoretically calculated profile of amorphous silica [39]. There is a difference between the electrochemical conversion of silica and silicon. During lithiation, silica can pass through ten 3-phase regions, which include silicon, lithium silicides and lithium silicates. In contrast to the monotonic voltage change during the reduction of amorphous phases, the crystalline phases of silica and silicon vary by steps.

Hollow nanospheres of silica for future LIA

Hollow nanospheres of silica with a uniform grain size close to 30 nm were successfully synthesized using a template from micelles of triblock copolymer ABC of poly-tyrene-b-2-vinylpyridine-b-ethylene oxide (PS−PVP−PEO) with core-shell architecture−crown [40]. In this type of copolymer, the PS unit (core) acts as a void template for hollow silica, the PVP unit (shell) acts as a reaction zone for the tetramethoxysilane sol-gel reaction (TMOS), and the PEO unit (crown) stabilizes the polymer/silica composite particles. The use of polymers with different chain lengths of PS, PVP and PEO has resulted in hollow silica with adjustable cavity size and wall thickness. The obtained hollow particles were carefully characterized by X-ray diffraction (XRD), thermal analysis (TG/DTA), nitrogen sorption, Fourier transform infrared spectroscopy (FTIR), nuclear magnetic resonance, and electron NMR, TEM. Empty silicon nanoparticles showed high indicators in LIA performance for 500 cycles. In the first cycle, the discharge capacity of hollow nanospheres reaches 980 mA·h·g^{-1}. Most of it is irreversible. The authors believe that after the first cycle of Li_2O/Si accumulation are distributed uniformly in the wall of the silica shell and prevent an increase in volume and/or reduction during charge/discharge. Hollow silica with a void diameter of 13.9±1.7 nm and a wall thickness of 5.8±0.4 nm showed capacitance values of 980, 472, 355, 359 and 336 mA·h·g^{-1} for the 1st, 2nd, 50th, 100th and 500th cycles, respectively. Similarly, the values of charge capacity were 323, 327, 336, 354 and 334 mA·h·g^{-1} for the 1st, 2nd, 50th, 100th and 500th cycles, respectively.

The inclusion of lithium in commercial dense silica powder (Alfa Esar, particle size about 10 μm) was studied. In the case of dense silica powder there is a drop in capacity during cycling. After 25 discharge-charge cycles, the retention capacity is 60% of the initial capacity, which is much smaller than the starting capacity of the hollow silica. High irreversible loss of active particle capacity was also

R.D. Apostolova, E.M. Shembel

observed in the case of dense silica compared to hollow silica nanospheres. The improvement in the cyclicity of hollow structures is mainly due to two factors. First, a hollow structure with a distinct cavity increases the mechanical stability of the electrodes. Second, the small grain size of the hollow nanospheres (30 nm) provides better electrical contact and a shorter diffusion path during the cycle, while maintaining the volume preserves the integrity of the electrode structure. Regarding the mechanism of formation of Li_2O/Si nanomatrix or nanocluster, the electrochemical reaction of SiO_x with Li^+ to obtain Li_2O and Si metal follows the equation:

$$SiO_x + 2xLi^+ + 2xe^- \leftrightarrow xLi_2O + Si. \qquad (13)$$

Li_2O formed in situ is known as an inactive matrix for the placement of active metal particles and as a good Li-ionic conductor. Li_2O/Si clusters are suitable for alloying processes during charging/discharging.

The effect of coating electrode materials for LIA with SiO_2 film

The surface coating of a number of electrode materials for LIA with a SiO_2 film has a positive effect on their electrochemical behavior in the redox reaction with lithium, in particular, natural graphite, $LiMn_2O_4$, $LiCoO_2$, and FeS.

SiO_2 film on natural graphite obtained using lithium tetraethylorthosilicate Si $(OCH_2CH_3)_4$ by the method of sol-gel process, followed by heat treatment in an argon atmosphere, improves the discharge characteristics of lithium batteries [41]. After 40 cycles, the reversible capacity of the modified graphite exceeds 366 $mA \cdot h \cdot g^{-1}$ with a Coulomb efficiency of 95.5% (83.04% for unmodified graphite). The modification helps to form a compact stable SEI surface film.

$LiMn_2O_4$ spinel samples were coated with 1.0 SiO_2 oxide; 2.0 and 3.0 wt.% using polymer method, followed by treatment at 850^0C for 6 hours in air [42]. The compact coating layer is about 50 nm. The loss of the discharge capacity of $LiMn_2O_4$ spinel coated with SiO_2 oxide (2.0 wt.%) was 4.8% of the initial capacity (126 $mA \cdot h \cdot g^{-1}$) in the 100th cycle at 30^0C and 8.9% at 60^0C. Based on the analysis of the results of electrochemical impedance spectroscopy, the improvement in cyclicity can be attributed to the transformation of the passive film and the reduction of Mn dissolution as a result of modification of the spinel surface of $LiMn_2O_4$ by SiO_2 dioxide.

Using a mixture of SiO_2 sol and lithium and cobalt acetate solution as precursors, nanometer SiO_2 modified $LiCoO_2$ films were made by electrostatic spraying [43]. The SiO_2 content in these films was 0, 5, 10, 15 and 20 wt.%. A film of 15 wt.% SiO_2 shows the best cyclic stability: a capacity of 130 $mA \cdot h \cdot g^{-1}$ in the voltage range from 2.7 to 4.3 V at a current density of 0.1 $mA \cdot cm^{-2}$, as well as excellent speed characteristics. A model of the $LiCoO_2$(shell)/SiO_2(core) structure is proposed to explain the improved properties of these films.

When comparing the discharge characteristics in the model lithium battery of electrochemically synthesized FeS sulfide and its composition with SiO_2, it was found that the discharge capacity of thin-film compositions (FeS, SiO_2) increases by 30−50% compared to that of thin-film FeS sulfide in the voltage range 2.8−1.1 V, as well as at 2.8−0.05 V vs. Li^+/Li electrode, which makes it possible to use them in the positive and negative electrodes of lithium-ion systems [44].

SiO_2 composites as promising materials for negative electrodes of next LIA generation

Many compositions have been proposed to improve the electrochemical properties of SiO_2. This review presents some promising developments from a number of SiO_2 compositions with nanotubes, carbon compounds, graphene, and mixtures of components.

Composite SiO_2@C/MWNT

Carbon-coated silica nanoparticles (2−7 nm) mounted on multi-walled carbon nanotubes (MWNT) were obtained as SiO_2@C/MWNT composite by a simple and easy sol-gel process followed by heat treatment [45]. The composition of the composite includes components in the ratio SiO_2:C:MWNT=77.5:17:5.5. Microscopy studies (SEM and TEM) confirmed the tight fixation of SiO_2 nanoparticles with carbon coating (C). The leading MWNT network, which facilitated the rapid transport of electrons and lithium ions, improves the structural stability of the composite. The SiO_2@C/MWNT composite showed a reversible capacity of 744 $mA \cdot h \cdot g^{-1}$ in the second discharge cycle at a current density of 100 $mA \cdot g^{-1}$ and excellent speed, which provides a capacity of 475 $mA \cdot h \cdot g^{-1}$ even at 1000 $mA \cdot g^{-1}$. Improvements of electrochemical processes of the triple composite anode SiO_2@C/MWNT are associated with its unique core-shell structure and strong synergistic effect between the individual components.

SiO_2@C/MWNT composites help to suppress side processes. The structure of the core/shell, the presence of multi-walled carbon nanotubes in the composite have an increased positive effect, which is manifested in increased discharge capacity,

compared with the composite $SiO_2@C$.

Porous SiO₂ composite with carbon coating as a suitable material for LIA

The main strategy for solving the problem of silica as an anode material was developed for the preparation of SiO_2 composites with carbon coating by carbonization in an argon atmosphere. A simple and environmentally friendly method of obtaining carbon-coated SiO_2 composites using sucrose as a carbon precursor in solutions with different concentrations was reported in ref. [46]. Nanometer SiO_2 was added to these solutions and sintered at 900^0C.

Carbon-coated SiO_2 composites were characterized by X-ray diffraction, X-ray photoelectron spectroscopy, thermogravimetry, transmission and scanning electron microscopy in combination with energy-dispersive X-ray spectroscopy, cyclic voltammetry. The calendered electrode C/SiO_2 (obtained from a sucrose solution of 0.085 M) shows the best cycle stability, capacity 714.3 mA·h·g^{-1}, high Coulomb efficiency, as well as the lowest resistance to charge transfer during 200 cycles without destruction of the electrodes. The improvement in electrochemical characteristics can be explained by the positive effect of a thin layer of carbon, which can effectively reduce the resistance between surfaces, inhibit the bulk expansion of the electrode during cycling.

The efficiency of cyclic voltammetry (CV) for both calendered and non-calendered electrodes was evaluated in a potential window of $0.001-3.0$ V with a scan rate of 0.1 mV·s^{-1} during the first three cycles. The cathode peak appears between 0 and 0.5 V, which is due to the process of SiO_2 lithiation. Two anode peaks can be observed at 0.45 V and 0.77 V in the second and third cycles, respectively, corresponding to the delithiation process.

Calendered electrodes show the following discharge capacity in the 5th cycle at 1 C for $C/SiO_2-0.04$ M, $C/SiO_2-0.055$ M and $C/SiO_2-0.085$ M: 591.5, 765.1 and 922.1 mA·h·g^{-1}, respectively. At the current density of C/10 for $C/SiO_2-0.04$ M, $C/SiO_2-0.055$ M and $C/SiO_2-0.085$ M, the discharge capacity reaches the values of 818.8, 1042.2 and 1231.3 mA·h·g^{-1}, respectively.

Composite SiO₂@carbon nanorod for LIA

To overcome the bulk expansion and increase the low electrical conductivity of silica, a composite of $SiO_2@$carbon nanorods with the formation of the core-shell structure was developed [47]. A light in situ coating strategy of polydopamine was used for the synthesis of a number of $SiO_2@$carbon nanorod composites with different thicknesses of carbon shells.

Carbon shell, evenly covered the surface of SiO_2 nanorods, to some extent inhibiting bulk expansion, as well as improving the electrical conductivity of SiO_2. The presence of micropores with a size of 0.68 nm and mesopores with a size of 8.6 to 29.5 nm was determined in the composite. High and stable reversible capacity at a current density of 100 mA·g^{-1} reaches 690 mA·h·g^{-1}, and a capacity of 344.9 mA·h·g^{-1} can be achieved even at a high current density of 1000 mA·g^{-1}. In addition, excellent capacity retention reaches 95% over 100 cycles. $SiO_2@$carbon nanorod composites with decent electrochemical characteristics have great potential for use in lithium-ion batteries.

Micro-sized porous composites C/SiO₂

Micro-sized porous C/SiO_2 composites were made from rice husk by a light carbonization process using $ZnCl_2$ as an activating agent in an Ar atmosphere [48]. C/SiO_2 demonstrates mesoporous morphology of particles with a specific surface area of 1191.30 m²·g^{-1}, high discharge capacity (approximately 1105 mA·h·g^{-1} at 0.1 A·g^{-1}), excellent cyclic stability and good speed in the anodes LIB. The porous structure can absorb volume changes and mechanical deformations, reduce the length of the lithium-ion diffusion path.

Silica in a composite with graphene oxide GO as a candidate for the negative electrodes of the LIA of the future

Graphene nanoplates are considered one of the most promising candidates for the production of high-performance anode material to replace graphite in lithium-ion batteries. Research in this field focuses mainly on nanostructured electrodes synthesized by the interaction of SiO_2 with graphene oxide (GO) or reduced graphene oxide (rGO), and surface modifications of SiO_2 by chemical treatment.

Hybrids ($SiO_2@$carbon-graphene oxide) with excellent electrochemical characteristics were obtained by self-assembly of colloidal silica, sucrose and graphene oxide, followed by hydrothermal and heat treatment using ultrasound [49]. The mass ratio of silica to sucrose is crucial for the electrochemical parameters of the obtained hybrids. The hybrid with a mass ratio of silica to sucrose of 0.15 shows the best reversible storage performance with lithium, providing an initial discharge capacity of 906 mA·h·g^{-1} and capacity 542 mA·h·g^{-1} in the 216th cycle at a current density of 100 mA·g^{-1}. Excellent cyclicity and high reversibility are explained by the synergistic effect of good conductivity of $SiO_2@$C-G hybrids, small SiO_2 particle size and good dispersion of SiO_2 nanoparticles in hybrids. This methodology can provide a simple, scalable and environmentally

friendly strategy for preparing excellent materials for electrodes from cheap and low-conductivity metal oxides.

The mechanism of the electrochemical reaction between SiO_2 and Li may depend on the microstructure [14,49]. Here, to better illustrate the mechanism of electrochemical reaction in SiO_2@C-GO hybrids, cyclic voltammograms (CVs) of SiO_2@C-GO electrodes were analyzed in the potential range of 0.005−2.500 V at a scan rate of 0.2 mV·s⁻¹. The CV profiles of different

SiO_2@C-GO hybrids are similar. In the first cycle on CVs of SiO_2@C-GO electrodes, large broad peaks in the range of 0.3−1.6 V change to small peaks, which become sharp with increasing ratio of silica to sucrose. This suggests that amorphous SiO_2 in SiO_2@C-GO hybrids may be active, involved in electrochemical reactions. Obviously, irreversible recovery peaks of about 0.75 V are associated with electrolyte decomposition and the formation of (SEI) on the electrode surface. The cathode peak below 0.5 V is associated with lithiation of SiO_2@C-GO hybrids, as described in reactions (1), (2), (3) and (14).

$$6C + yLi^+ + ye^- \leftrightarrow Li_yC_6 \qquad (14)$$

With increasing mass ratio of silica/sucrose, the anode peak with a center of 0.2 V becomes narrow and indicates the process of extraction of Li from the formed alloy Li_xSi. Carbon component and in situ formed electrochemically active Si, contribute a certain amount of reversible capacity (equations (3) and (14)) during reversible lithiation/ delithiation of composite. From the second cycle, the CV curves become almost stable and show mainly the reversible behavior of amorphous silicon and disordered carbon (equations (3) and (14)), which assumes satisfactory performance of SiO_2@C-GO hybrids.

Hollow sandwich-like structures of silicon oxides with carbon as a material for negative electrodes LIA

Hollow sandwich-like structures were developed and N-doped carbon−silica−carbon composite (CSC) fabricated as anode materials for LIB [50]. The combination of polymer template and polymerization of dopamine self-oxidation leads to the formation of conformational coatings on the surface of silica, which increases the conductivity and stability of composite materials. The material with a hollow sandwich structure shows a high reversible capacity of 480 mA·h·g⁻¹ at a current density of 1.0 A·g⁻¹ and excellent speed, which can be explained by the synergistic effect of the unique structure of hollow silica and N-doped carbon

conformational coating. Composite materials made of hollow sandwich-structured components (N-doped carbon-silica-carbon) can be promising anode materials for LIB.

Electrodes for LIA were prepared by mixing 70 wt.% active materials (CSC), 20 wt.% Super P as a leading agent and 10 wt.% polyvinylidene fluoride (PVDF) as a binder. The electrolyte was 1 M $LiPF_6$ in a mixture of 1:1 (vol./vol.) ethylene carbonate (EC) and dimethyl carbonate (DMC), the separator was a Celgard 2400 membrane. According to XRD composite CSC, the structure of hollow silica is amorphous. Composites are characterized by a hollow sphere, well dispersed and homogeneous with a diameter of less than 100 nm.

The mechanism of electrochemical reactions of the composite with lithium ion was determined, which is described by equations (2), (3), (9) and (15) [51,52].

$$2SiO_2 + 2Li^+ + 2e^- \rightarrow Li_2O_4 + 2Si \qquad (15)$$

On cyclic voltammograms of CSC nanocomposites at a potential scan rate of 0.1 mV·s⁻¹ in the range of 0.01−3.00 V, there are two peaks at 0.75 and 0.20 V; peak at 0.75 V due to irreversible reactions between the electrode and electrolyte and the continuation of film formation SEI [53]. The peak at 0.2 V is related to the inverse reaction of silicon fusion with Li ions (equation (3)). The CV curves in the carbon-silica-carbon composite almost overlap during cycling, indicating extremely reversible behavior. Discharge and charge voltage profiles at a current density of 1.0 A·g⁻¹ in the voltage range of 0.2−3.0 V are in good agreement with the CV measurements. In the first discharge voltage profile, a plateau was observed at 0.7 V, which can be explained by the formation of SEI and the irreversible reaction of the silica electrode with the electrolyte. The discharge and charge capacities of the first cycle are 1080 and 450 mA·h·g⁻¹ at 1.0 A·g⁻¹ with initial CE 42%. Long-term cycling at 1.0 A·g⁻¹ indicates a return capacity of 500 mA·h·g⁻¹ even after 700 cycles with a high CE, approaching 100%. Excellent electrochemical performance can be attributed to the unique sandwich structure, which plays an important role in achieving excellent structural stability and stable cycling. The silica cavity and protective gap can counteract bulky changes during cycling and stabilize the structure.

Mechanism of chemical and electrochemical interaction of SiO oxide with lithium

Silicon oxide (SiO), consisting of nanosized Si

and amorphous matrix SiO_2, attracts as an anode material with a high theoretical capacity (2100 mA·h·g^{-1}), which is 5 times more than graphite [54,55]. The amorphous component of SiO_2 in the SiO matrix can release a large change in volume, the Si component is effective during charging (inclusion of Li$^+$) during cycling. However, the amorphous component of α-SiO_2 in the SiO matrix changes irreversibly to lithium silicate [56]. The reaction mechanism of SiO with Li is summarized by the following reaction:

$$4SiO + 17.2Li \rightarrow 3Li_{4.4}Si + Li_4SiO_4. \qquad (16)$$

Li_4SiO_4 is the reaction product of the amorphous component a-SiO_2 in the SiO matrix with Li during the first charge process. Some SiO bonds are broken by lithium, but some SiO bonds still remain to form Li_4SiO_4. Based on (XPS), it was determined that formed after the first charge lithium silicate can be partially delithiated in the next discharge process [57]. This means that the reversible part and the irreversible part coexist in an amorphous silicon oxide matrix. In addition, it was reported that crystalline SiO_2 (Tridymite; MKHD No. 00-089-3608), deposited by radio frequency sputtering, after cycling was converted to $Li_2Si_2O_5$ and it became possible to reverse the conversion of tridymites SiO_2 with Li [28]. In this case, the bonds in the silicon oxide SiO are not permanently broken.

The activity of silicon dioxide with Li was determined by chemical and electrochemical reactions in the study [54]. Additionally, the energy of formation was calculated according to the theory of the first principles to confirm the possibility of the reaction of silicon dioxide with Li. The suspension for the working electrode was prepared by mixing crystalline or amorphous SiO_2 as active material with acetylene black as an electronic conductor and with polyimide as a binder in a weight ratio of 76.5:13.5:10 in a solution of N-methylpyrrolidone (NMP). The electrolyte was 1 M LiPF$_6$, ethylene carbonate (EC) and diethyl carbonate (DEC) in a ratio of 3:7.

The electrochemical reaction was measured in the voltage range from 0.01 to 1.2 V vs. Li$^+$/Li at the speed of 0.025 mA·cm^{-2} at 60^{0}C. In the case of chemical interaction SiO with lithium, silicon with a particle diameter of 3 nm and amorphous SiO_2 were found in the starting material. After interaction with lithium, the presence of Li_2SiO_3, Li_4SiO_4, $Li_{22}Si_5$ was detected. Li_4SiO_4 must be formed by the reaction of the amorphous component SiO_2 in the SiO matrix with lithium.

Crystalline quartz SiO_2 retained the structure with the space group P3121 after reaction with Li. Based on the above data, that crystalline SiO_2 and Li_4SiO_4 did not react chemically with Li, it can be concluded that SiO bonds in SiO_4 tetrahedra, which are mainly structural units in silicon dioxide, were not easily broken by lithium.

The charge-discharge curves of the electrochemical interaction of SiO with lithium show inclined plateaus at 0.5 V and 0.2 V vs. Li$^+$/Li, which are associated with the interaction Li with amorphous SiO_2 in SiO and one of Si with Li formatting Li_xSi alloy. The charge and subsequent discharge capacity of SiO were 2548 and 1791 mA·h·g^{-1}.

The electrochemical activity of amorphous and crystalline SiO_2 was also investigated by testing the charge-discharge process with a Li-metal anode. The voltage plateau was observed at 0.05 V against Li$^+$/Li in the case of amorphous silica. This plateau indicated the reaction of amorphous SiO_2 with Li. The first charge and subsequent capacity for the discharge of amorphous SiO_2 was 2013 and 950 mA·h·g^{-1}, respectively. Although amorphous SiO_2 can react reversibly with lithium, crystalline quartz cannot. Electrochemical activity of crystalline Li_4SiO_4 was not manifested.

According to experimental results and theoretical calculations, one of the triggers for the irreversible reaction to SiO is distorted SiO_4 tetrahedra in amorphous SiO_2, due to the possibility of reducing the non-equivalent bond length of SiO_4 tetrahedra in silicon oxide with the help of lithium.

Prelithiation as a way to solve the problem of loss of SiO_2 capacity during cycling

Prelithiation is an important strategy used to compensate for lithium losses during solid electrolyte (SEI) formation and other irreversible reactions in the first stage of the electrochemical cycle. In [57], a systematic study of thermal prelithiation of SiO_2 particles of different sizes (6 nm, 20 nm, 300 nm and 3 mm) was reported. All four lithium anodes (Li_xSi/Li_2O composites) show improved performance compared to virgin SiO_2. They exhibit optimum performance with a starting charging capacity of 1859 mA·h·g^{-1} and over 1300 mA·h·g^{-1} for more than 50 cycles.

It was shown that silica can form a number of irreversible lithium silicates and Li_2O in the first cycle during lithiation. This process consumes an excessive amount of cathode materials, which significantly reduces the total energy density of complete elements, thereby preventing their practical application. To solve this problem, the researchers proposed prelithiated electrode material, which directly compensates for the irreversible loss of lithium during

R.D. Apostolova, E.M. Shembel

the first cycle [58−61].

Here we present the prelithiated composites ($Li_xSi/L_{i2}O$) proposed in the work [62]. Such composites have numerous advantages as follows: (1) prelithiation effectively improves the electrical conductivity of silica, facilitating its functioning as an anode with high capacity and cycle stability; (2) Li_xSi/Li_2O composites can solve the problem of Si-based low Coulomb efficiency (CE) anodes, which is a huge challenge for practical applications; and (3) the Li_xSi/Li_2O composite alloy can serve as a promising lithium-containing anode for coupling to high-capacity lithium-free cathodes, such as S, for next-generation lithium-ion batteries.

SiO_2 particles of different sizes (6 nm, 20 nm, 300 nm and 3 μm) were selected for systematic determination of electrochemical characteristics. All prelithiated composites labeled Li_xSi/Li_2O-1, Li_xSi/Li_2O-2, Li_xSi/Li_2O-3 and Li_xSi/Li_2O-4, which correspond to different sizes of virgin SiO_2 particles, show better performance than virgin SiO_2 particles. More interestingly, the prelithiated composite of SiO_2 microparticles demonstrates the best cycle stability, reaching an initial capacity of 1859 mA·h·g^{-1} and maintaining above 1300 mA·h·g^{-1} after 50 cycles.

Electrochemical properties were determined using CR 2032-coin cells. The active material was mixed with acetylene carbon black and carboxymethylcellulose (CMC) (weight ratio 65:20:15) in tetrahydrofuran (THF) to form a suspension. Then the suspension was evenly coated on copper foil. The mass load of the suspension on each copper foil (diameter of 12 mm) is approximately 0.3−3.5 mg. The electrodes were assembled in a glove box filled with Ar, using lithium foil as a counter electrode and Celgard 2300 film as a separator. An electrolyte solution consisting of 1 M $LiPF_6$ dissolved in ethylene carbonate (EC), dimethyl carbonate (DMC) (1:1 by volume) was used to collect the cells. Measurements in galvanostatic charge-discharge processes were tested between 0.01 and 1.0 V at a speed of 0.05 C on a tester (LAND CT2001A, Wuhan, China). Cyclic voltammetry (CV) was performed on an electrochemical workstation (Bio-logic VMP3) with a potential scan rate of 0.1 mV·s^{-1} in the potential range from 0.01 to 3.00 V. After lithiation, nanoparticles tend to aggregate into microparticles, while micro- or submicro-particles prefer to retain their size during the lithiation process. According to the XRD, the presence of Li_2O and $Li_{21}Si_5$ in prelithiated SiO_2 particles has been shown, demonstrating the formation of Li_2O (PDF # 04-001-893) and $Li_{21}Si_5$ phases (PDF # 00-018-747). The crystal sizes of the four composites are 28.2,

29.3, 31.9 and 37.5 nm, which indicates the formation of relatively large $Li_{21}Si_5$ domains.

All lithiated SiO_2 electrodes have similar plateaus of about 0.45 V, which indicates the same active materials (Li_xSi) of the electrodes and their high crystallinity. Capacities for prelithiated SiO_2 particles are 1972, 2267, 1776 and 1412 mA·h·g^{-1} according to particle size. Thermal prelithiation can effectively compensate for the huge irreversible loss of lithium during the first cycles by the formation of lithium silicates and Li_2O. Cyclic voltammetry tests were performed for both virgin and prelithiated SiO_2 oxides for 3 consecutive cycles from 3.00 V to 0.01 V at a scan rate of 0.05 mV·s^{-1}. In the first cycle, the prelithiated SiO_2 electrode exhibits cathode peaks above 1.0 V, which corresponds to irreversible electrochemical reactions between SiO_2 and Li, which disappear in subsequent cycles. The cathode peak below 0.2 V is attributed to the process of silicon lithiation. The electrochemical process involved are described by the equations (1), (2) and (9).

The cathode peak at 0.5 V in the first cycle confirms the formation of highly crystalline Li_xSi. The two clear anode peaks around 0.34 and 0.51 V during the second and third cycles are consistent with the characteristic peaks of the division process from amorphous Li_xSi to Si. The electrochemical equation is proposed as Eq. (3).

The prelithiated sample provides a fast path for electron transport between Li domains.

Hybrid SiO_2/metal for negative electrodes LIA

Hybrid anode materials SiO_2/conductive metal demonstrate improved electrical conductivity and increased electrochemical activity in electrochemical interaction with lithium. Thus, Zhou, Mei, and co-workers created a SiO_2/Ni nanocomposite with a hierarchical hollow spherical structure by synthesizing nickel silicate followed by its reduction in an H_2/Ar atmosphere (5%/95%, respectively) [63]. The unique structured SiO_2/Ni nanocomposite is constructed of ultrathin Ni nanoparticles (≈3 nm) and SiO_2 nanoleaves. Ni nanoparticles increase not only the electronic conductivity but also the electrochemical activity of efficient use of SiO_2. Meanwhile, the cavity provides enough free space to accommodate the change in SiO_2 volume during relithiation/delithiation; nanoleaf building blocks reduce the diffusion length of lithium ions. The obtained SiO_2/Ni nanocomposite has the following structural characteristics, qualities for lithium storage: (I) hollow spherical structure for accommodation of volume fluctuations and stress relaxation; (II) ultrathin nanosheet building blocks for efficient Li$^+$ diffusion; and (III) framing of ultrafine Ni nanoparticles to

improve electron transfer. Due to these unique design features, the hierarchical hollow spheres of SiO_2/Ni demonstrated a high specific capacity of 672 mA·h·g^{-1} after 50 cycles at 100 mA·g^{-1} and 337 mA·h·g^{-1} after 1000 cycles at a current density of 10 A·g^{-1}.

The characteristics of the SiO_2/Ni nanocomposite in the electrochemical interaction with lithium differ significantly in the first cycle from those in subsequent cycles. The discharge curve in the first cycle has two inclined horizontal sections of potentials of 1.4 and 0.75 V, which disappear in subsequent cycles. The authors attribute them, referring to the literature, to the interaction of silica with lithium at 1.4 V and the decomposition of the electrolyte to form a SEI film at 0.65 V. It is believed that a wide peak around 1.4 V can be described by reactions with the formation of $Li_2Si_2O_5$, Li_2O, Li_4SiO_4. The current peak in the range of 0.25−0 V on the CV is attributed to the processes of alloying Li_xSi.

The positive effect of nickel on the electrochemical behavior of silicon dioxide in the composition of the SiO_2/Ni composite is evidenced by the increase in the discharge capacity of the composite by 3.5−4.0 times relative to the discharge capacity of SiO_2.

Hybrid SiO_2@carbon-graphene (SiO_2@C-Gr) as a material for negative electrodes LIA

Hybrids of SiO_2@carbon-graphene (SiO_2@C-Gr) with excellent electrochemical characteristics were prepared by self-assembly of colloidal silica, sucrose and graphene oxide, followed by hydrothermal and heat treatment using ultrasound [64]. The mass ratio of silica to sucrose is crucial for the electrochemical characteristics of the obtained hybrids. The best ratio of silica to sucrose 0.15 provides an initial discharge capacity of 906 mA·h·g^{-1} and a capacity of 542 mA·h·g^{-1} on the 216th cycle at a current density of 100 mA·g^{-1}.

The excellent long cycling ability and high reversibility are explained by the synergistic effect of carbon with graphene, small SiO_2 particle size and good dispersion of SiO_2 nanoparticles in hybrids. This methodology can provide a simple, scalable and environmentally friendly strategy for the preparation of electrode materials from cheap metal oxides with low electrical conductivity.

SiO_2@Sn composite as a material for LIA negative electrodes

The development of anode materials based on SiO_2 for LIA is hindered by their poor electrical conductivity and slow kinetics of charge transfer. In this case, porous composites SiO_2/tin (SiO_2@Sn) with different molar ratio of SiO_2 to Sn are made using a scalable, simple and inexpensive combined method of ball mill and low-temperature thermal melting to solve these problems [65]. It was found that the Sn phase can significantly improve the kinetics of diffusion and migration of Li ions in composites, while the molar ratio of SiO_2 to Sn plays a key role in the mechanical integrity and subsequent cyclic behavior of composite electrodes. By optimizing the SiO_2/Sn molar ratio to 10:1, the synergistic effect of Li storage between SiO_2 and Sn can simultaneously lead to improved Li kinetics and mechanical integrity, contributing to the excellent electrochemical characteristics of the composite with a return capacity of 613 mA·h·g^{-1} at 100 mA·g^{-1}, excellent ability to maintain capacity up to 450 mA·h·g^{-1} at 1000 mA·g^{-1} and durability of cycling while maintaining capacity ≈95% for 200 cycles.

Prospects of a-SiO_2/FeSi/G composite as a material for LIA negative electrodes

To develop high-efficiency anodes based on amorphous a-SiO_2 dioxide for lithium-ion batteries, amorphous a-SiO_2-FeSi-graphite composite (a-SiO_2/FeSi/G) was synthesized using an energy-intensive ball mill from a mixture of amorphous silica and powder (mesoporous MSMV) [66]. The a-SiO_2/FeSi/G composite consists of amorphous SiO_2, an inactive FeSi matrix (particle size of 5−10 nm) inside a graphite matrix. The a-SiO_2/FeSi/G composite electrode demonstrated electrochemical properties with a high initial charge capacity of 729 mA·h·g^{-1}, with a high initial Coulomb efficiency of approximately 74%, and a long retention capacity of 93.7% after 200 cycles, with a high reverse capacity 683 mA·h·g^{-1}.

The discharge-charging characteristics of the a-SiO_2/FeSi/G composite are characterized by the absence of significant side processes of electrolyte decomposition in the first cycle. A slight common peak of current is observed only at 0.75−0.80 V. Current peaks occur at 0.20−0.25 V in the region of interaction of SiO_2 with lithium, the region of alloying Li_xSi.

Discussion and conclusions

Data from the sources of information provided in the review shows the possibility of influencing the electrochemical behavior of silicon, the most promising anode material for the negative electrodes of future LIA, by modifying the surface of the silicon electrode. Therefore, it is important to optimize the quality of the Si-base compound in order to: (i) improve the properties of the silicon electrode, and (ii) use the Si-oxide compound as a stand-alone material for negative electrodes LIA.

The first part of the review focuses on the

determination of promising silicon dioxide SiO_2 of various modifications and structural organization. The electrochemical parameters of SiO_2 dioxide-crystalline and amorphous in the formats of thin films, pyrogenically obtained particles, encapsulated in Ni-matrix by electrolysis, hollow porous SiO_2 nanoparticles, nanotubes, nanowires and hollow nanospheres have been compared.

The second part of the review considers the features of electrochemical conversion of SiO_2 in composites with multi-walled carbon nanotubes, porous silica with carbon coating, in the composite with carbon nano-rods, in the composite with graphene oxide, in the composite with Sn, the composite with FeSi, monoxide with a composition of $Si+SiO_2$, prelithiated silica, in a composition with nickel, and in composites SiO_2/carbon/graphene. Unfortunately, this does not include metal-organic compounds, which are identified as promising in the study of electrode materials, but not widely tested with SiO_2 [67].

These data showed varying degrees of electrochemical inverse transformation in redox reaction with lithium.

Analysis of discharge-charge curves and cyclic voltammograms of SiO_2 in redox reactions with lithium shows the distribution of materials into two groups. In the first group, the electrode process continues mainly in the region of low potentials: below 0.4 V relative to the Li^+/Li electrode [14,24,54]. In this case, the recovery curve has a profile similar to that shown in Fig. 3. In the second group, along with the characteristics of low-voltage conversion, the electrode is also transformed within higher values of the potentials of the electrode, clearly expressed in ref. [27,34,40,47,63], the profile of the recovery curves of which is shown in Fig. 4. In this case, most often these signs of transformation within the higher values of the electrode potentials disappear in the second and subsequent cycles.

A significant number of studies of SiO_2 and Si have been conducted using modern instrumental methods and it has been determined that the reduction processes at potentials of 0.90−0.65 V relate to the decomposition of the electrolyte with the formation of the SEI surface film. Si, Li_2O, Li_xSi silicates are formed after reaching a potential below 0.5−0.4 V. However, the interpretation of the mechanism of the obtained curves by different authors is ambiguous and sometimes does not coincide with the proposed and experimentally confirmed mechanism. Thus, we may not agree with the interpretation of the results of the study of the thin-film composite SiO_2/Ni [27]. The reduction process
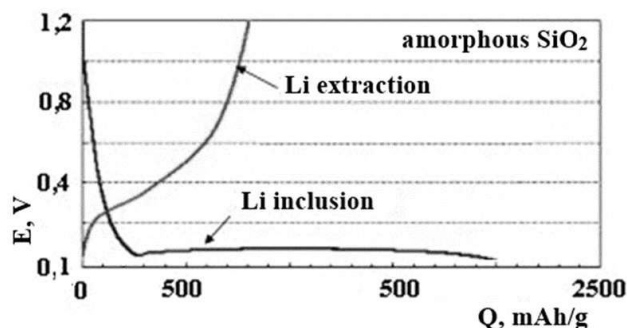
Fig. 3. Typical possible profile of the curves for groups Si-1
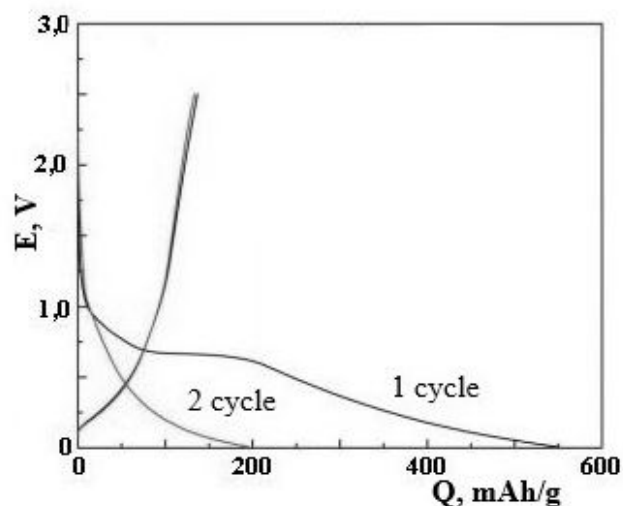
Fig. 4. Typical possible profile of the curves for groups Si-2

of SiO_2/Ni at 1.4 V is described by the interaction of silicon dioxide with lithium with the formation of $Li_2Si_2O_5$, Li_2O, Li_4SiO_4. In the case of electrolytically encapsulated silicon dioxide with nickel, similar processes were observed around 1.4 and 0.75 V [24]. A separate study of the nickel base in the electrochemical interaction with lithium was conducted. The participation of nickel oxides that exist on the surface of nickel in the redox reaction with lithium was shown. Apostolova et al. [24] identified the process at the peak position of 1.4 V in a thin-layer a-SiO_2/Ni composite as a process of reducing Ni-oxide film on the surface of the nickel base of the electrode. The reduction of the Ni-oxide film is damaged and becomes irreversible in the second cycle. In addition, the reaction of formation of lithium silicate $Li_2Si_2O_5$ at the beginning of the cycling of silicon dioxide is considered to be the opposite in many studies, and it occurs at potentials below 0.4−0.5 V relative to Li^+/Li.

The question arises how to explain the

difference in the electrochemical behavior of samples from group 1 and group 2. It should be sought in the experimental conditions. In the case of group 1, the method of obtaining the studied silicon dioxide by grinding in an energy-intensive ball mill without contact with the electrolyte [14,54] and the method of encapsulating silicon dioxide with nickel [24] were used. These methods allow limiting the negative impact of the electrolyte with contamination of the interface of silicon dioxide with impurities. SiO_2 samples from group 2 were obtained by methods that continue in bulk electrolyte solution. A significant share of irreversible processes of conversion of silicon dioxide with lithium is due to side processes occurring on the electrode surface with oxide film, sensitive to impurities from electrolyte and silicon dioxide contaminated with electrolyte as a result of adsorption, ion exchange and other processes.

The efficiency of electrochemical conversion of the electrode material is known to be determined by the processes associated with the SEI surface film and the retention of lithium ions in the space of the electrode. The difference between the lithium characteristics of the SiO_2 samples of the two groups is due to the different behavior of the SEI film. It is formed in the first cycle with inefficient energy consumption, due to which the discharge capacity of the current source SiO_2/Li can be lost by almost 50%. Such a significant loss is not observed in the group of amorphous dioxides a-SiO_2, which was obtained by grinding in a ball mill. It is known that the electrode materials synthesized in the ball mill are less contaminated with impurities than synthesized in solutions. Similarly, the encapsulation of nickel by silica synthesized by electrolysis reduces the expected contamination due to the limited contact of SiO_2 with the bulk electrolyte.

In the synthesis of silica in solutions, the possibility of contamination of the final product increases due to adsorption processes, especially when using several reagents in multi-stage synthesis technology. Unfortunately, the lack of control of the synthesized material for purity makes it difficult to identify the causes of degradation of the lithium process and make further recommendations. It is necessary to systematize the experimental material in the main areas of study of the qualities of silica obtained by different methods.

In studies of too thin silica films, the authors did not pay attention to the preparation of the electrode substrate and it is not about cleaning the surface. For research in thin films, there are many methods of surface cleaning. The authors sometimes take side processes on the surface of the thin-walled substrate as a significant main electrode process.

When comparing the electrochemical characteristics of silica of different formats, a clear advantage is not observed. The lithium characteristics obtained by different authors by the same method differ. In addition, cycling results are not easy to evaluate when they are obtained at different current densities with different number of cycles.

Some of our comments made in the review can be taken as recommendations for improving the performance of silicon dioxide in LIA.

REFERENCES

1. *Electrochemical* characteristics of $Sn_{1-x}Si_xO_2$ as anode for lithium-ion batteries / Huang H., Kelder E.M., Chen L., Schoonman J. // J. Power Sources. − 1999. − Vol.81-82. − P.362-367.

2. *Towards* a fundamental understanding of the improved electrochemical performance of silicon-carbon composites / Saint J., Moncrette M., Larcher D., Laffont L., Beattie S., Peres J.P., et al. // Adv. Funct. Mater. − 2007. − Vol.17. − P.1765-1774.

3. *Obrovac M.N., Christensen L.* Structural changes in silicon anodes during lithium insertion/extraction // Electrochem. Solid-State Lett. − 2004. − Vol.7. − P.A93.

4. *Silicon* oxides: a promising family of anode materials for lithium-ion batteries / Liu Z., Yu Q., Zhao Y., He R., Xu M., Feng S., et al. // Chem. Soc. Rev. − 2019. − Vol.48. − P.285-309.

5. *Apostolova R.D., Zaderey N.D., Kirsanova I.V.* Reshenie problem povysheniya energoemkosti i stabilnosti tsiklirovaniya Si-, SiO-, SiO-elektrodov dlya litiy-ionnykh istochnikov toka: analiticheskiy obzor // Voprosy Khimii i Khimicheskoi Tekhnologii. − 2016. − No. 5-6. − P.31-52.

6. *Lithiation* of silica through partial reduction / Ban C., Kappes B.B., Xu Q., Engtrakul C., Ciobanu C.V., Dillon A.C., et al. // Appl. Phys. Lett. − 2012. − Vol.100. − Art. No. 243905.

7. *Lithiation* of SiO_2 in Li-ion batteries: in situ transmission electron microscopy experiments and theoretical studies / Zhang Y., Li Y., Wang Z., Zhao K. // Nano Lett. − 2014. − Vol.14. − P.7161-7170.

8. *Perez-Beltran S., Ramirez-Caballero G.E., Balbuena P.B.* First-principles calculations of lithiation of a hydroxylated surface of amorphous silicon dioxide // J. Phys. Chem. C. − 2015. − Vol.119. − P.16424-16431.

9. *Atomic* insight into the lithium storage and diffusion mechanism of SiO_2/Al_2O_3 electrodes of lithium ion batteries: Reax FF reactive force field modeling / Ostadhossein A., Kim S.Y., Cubuk E.D., Qi Y., van Duin A.C.T. // J. Phys. Chem. A. − 2016. − Vol.120. − P.2114-2127.

10. *Energetics* of silica lithiation and its applications to lithium ion batteries / Lener G., Otero M., Barraco D.E., Leiva E.P.M. // Electrochim. Acta. − 2018. − Vol.259. − P.1053-

1058.

11. *Electrochemical* reduction of nano-SiO_2 in hard carbon as anode material for lithium ion batteries / Guo B., Shu J., Wang Z., Yang H., Shi L., Liu Y., et al. // Electrochem. Commun. − 2008. − Vol.10. − P.1876-1878.

12. *Highly* reversible lithium storage in nanostructured silicon / Graetz J., Ahn C.C., Yazami R., Fultz Z. // Electrochem. Solid-State Lett. − 2003. − Vol.6. − P.A194.

13. *Termodinamichni* osoblyvosti strumoutvoruyuchogo protsesu v litiyevykh dzherelakh strumu z katodom na osnovi pirogennogo dioksydu kremniyu / Mironjuk I.F., Ogenko V.M., Ostafejchuk B.K., Mandzjuk V.I., Grigorchuk I.I. // Fizika i Khimiya Tverdogo Tila. − 2001. − Vol.2. − P.661.

14. *Quartz* (SiO_2): a new energy storage anode material for Li-ion batteries / Chang W.S., Park C.M., Kim J.H., Kim Y.U., Jeong G., Sohn H.J. // Energy Environ. Sci. − 2012. − Vol.5. − P.6895-6899.

15. *Guo Y.G., Hu J.S., Wan L.J.* Nanostructured materials for electrochemical energy conversion and storage devices // Adv. Mater. − 2008. − Vol.20. − P.2878-2887.

16. *Bruce P.G., Scrosati B., Tarascon J.M.* Nanomaterials for rechargeable lithium batteries // Angew. Chem. Int. Ed. − 2008. − Vol.47. − P.2930-2946.

17. *SiO_2/N-doped* graphene aerogel composite anode for lithium-ion batteries / Dong X., Zheng X., Deng Y., Wang L., Hong H., Ju Z. // J. Mater. Sci. − 2020. − Vol.55. − P.13023-13035.

18. *Sun Y., Liu N., Cui Y.* Promises and challenges of nanomaterials for lithium-based rechargeable batteries // Nat. Energy. − 2016. − Vol.1. − Art. No. 16071.

19. *Phase* relations of Li_2O−FeO−SiO_2 ternary system and electrochemical properties of $Li_xSi_yO_z$ compounds / Yan D., Geng X., Zhao Y., Lin X., Liu X. // J. Mater. Sci. − 2016. − Vol.51. − P.6452-6463.

20. *Surface* oxidation of nano-silicon as a method for cycle life enhancement of Li-ion active materials / Ratynski M., Hamankiewicz B., Buchberger A.D., Czerwinski A. // Molecules. − 2020. − Vol.25. − Art. No.4093.

21. *Enhanced* interfacial stability of Si anodes for Li-ion batteries via surface SiO_2 coating / Schnabel M., Arca E., Ha Y., Stetson C., Teeter G., Han S.D., et al. // ACS Appl. Energy Mater. − 2020. − Vol.3. − P.8842-8849.

22. *The effects* of native oxides surface layer on the electrochemical performance of Si nanoparticle-based electrodes / Xun S., Song X., Wang L., Grass M.E., Liu Z., Battaglia V.S., et al. // J. Electrochem. Soc. − 2011. − Vol.158. − P.A1260.

23. *Moon J., Park M.S., Cho M.* Anisotropic compositional expansion and chemical potential of lithiated SiO_2 electrodes: multiscale mechanical analysis // ACS Appl. Mater. Interfaces. − 2019. − Vol.11. − P.19183-19190.

24. *Thin-layer* electrochemically produced SiO_2/Ni composites in a prototyping lithium-ion battery / Apostolova R.D., Matsievskii N.A., Gladun V.A., Savchenko M.O. // Surf. Eng. Appl. Electrochem. − 2018. − Vol.54. − P.420-426.

25. *Apostolova R.D., Nagirnyi V.M., Shembel E.M.* Razrabotka i issledovaniye katodnogo materiala $LiCoO_2$ na osnove elektroliticheskogo oksida kobalta // Russ. J. Electrochem. − 1998. − Vol.34. − P.778.

26. *Otritsatelnye* elektrody dlya litii-ionnykh akumulatorov na osnove poristogo kremniya / Astrova E.V., Fjedulova G.V., Smirnova I.A., Remenjuk A.D., Kulova T.L., Skundin A.M. // Pisma v Zhurnal Tekhnicheskoi Fiziki. − 2011. − Vol.37. − P.87.

27. *Sun Q., Zhang B., Fu Z.W.* Lithium electrochemistry of SiO_2 thin film electrode for lithium-ion batteries // Appl. Surf. Sci. − 2008. − Vol.254. − P.3774-3779.

28. *Electrochemically-driven* solid-state amorphization in lithium-silicon alloys and implications for lithium storage / Limthongkul P., Jang Y.I., Dudeny N.J., Chiang Y.M. // Acta Mater. − 2003. − Vol.51. − P.1103-1113.

29. *SiO_x-based* anodes for secondary lithium batteries / Yang J., Takeda Y., Imanishi N., Capiglia C., Xie J.Y., Yamamoto O. // Solid State Ionics. − 2002. − Vol.152-153. − P.125-129.

30. *Analysis* of SiO anodes for lithium-ion batteries / Miyachi M., Yamamoto H., Kawai H., Ohta T., Shirakata M. // J. Electrochem. Soc. − 2005. − Vol.152. − P.A2089-A2091.

31. *Nanoporous* tree-like SiO_2 films fabricated by sol-gel assisted electrostatic spray deposition / Li X., Dhanabalan A., Meng X., Gu L., Sun X., Wang C. // Microporous Mesoporous Mater. − 2012. − Vol.151. − P.488-494.

32. *Carbon-coated* SiO_2 nanoparticles as anode material for lithium ion batteries / Yao Y., Zhang J., Xue L., Huang T., Yu A. // J. Power Sources. − 2011. − Vol.196. − P.10240-10243.

33. *Hydrothermal* synthesis and electrochemical performance of amorphous SiO_2 nanospheres/graphene composites / Yang Y., Gao Y., Liu J., Fang X. // Mater. Sci. Appl. − 2017. − Vol.8. − P.959-965.

34. *Stable* cycling of SiO_2 nanotubes as high-performance anodes for lithium-ion batteries / Favors Z., Wang W., Bay H.H., George A., Ozkan M., Ozkan C.S. // Sci. Rep. − 2014. − Vol.4. Art. No. 4605.

35. *In situ* synthesis of silica/graphite anode material with enhanced lithium storage performance / Liang J., Yang S., Ye L., Li X., Yang X., Chen S., et al. // J. Mater. Sci. Mater. Electron. − 2021. − Vol.32. − P.28119-28128.

36. *Hollow* porous SiO_2 nanocubes towards high-performance anodes for lithium-ion batteries / Yan N., Wang F., Zhong H., Li Y., Wang Y., Hu L., et al. // Sci. Rep. − 2013. − Vol.3. − Art. No. 1568.

37. *Carbon-coated* SiO_2 nanoparticles as anode material for lithium ion batteries / Yao Y., Zhang J., Xue L., Huang T., Yu A. // J. Power Sources. − 2011. − Vol.196. − P.10240-10243.

38. *Preparation* of SiO_2 nanowire arrays as anode material with enhanced lithium storage performance / Li W., Wang F., Ma M., Zhou J., Liu Y., Chen Y. // RSC Adv. − 2018. − Vol.8. − P.33652-33658.

39. *Sivonxay E., Aykol M., Persson K.A.* The lithiation process and Li diffusion in amorphous SiO_2 and Si from first-principles // Electrochim. Acta. 2020. − Vol.331. − Art.

No. 135344.

40. *Synthesis*, characterization and application for lithium-ion rechargeable batteries of hollow silica nanospheres / Sasidharan M., Liu D., Gunawardhana N., Yoshio M., Nakashima K. // J. Mater. Chem. − 2011. − Vol.21. − P.13881-13888.

41. *Preparation* and lithium-storage performance of carbon/silica composite with a unique porous bicontinuous nanostructure / Yang X., Huang H., Li Z., Zhong M., Zhang G., Wu D. // Carbon. − 2014. − Vol.77. − P.275-280.

42. *Arumugam D., Kalaignan G.P.* Synthesis and electrochemical characterizations of nano-SiO_2-coated $LiMn_2O_4$ cathode materials for rechargeable lithium batteries // J. Electroanal. Chem. − 2008. − Vol.624. − P.197-204.

43. *Electrochemical* performance of nano-SiO_2 modified $LiCoO_2$ thin films fabricated by electrostatic spray deposition (ESD) / Yu Y., Shui J.L., Jin Y., Chen C.H. // Electrochim. Acta. − 2006. − Vol.51. − P.3292-3296.

44. *Improvement* of FeS characteristics in Li accumulators by electrochemical codeposition with SiO_2 / Matzijevskiy N.A., Apostolova R.D., Savchenko M.O., Gladun A. // Promising materials and processes in technical electrochemistry. − Kyiv: KNUTD Publishers, 2016. P.68-73.

45. *Facile* synthesis of SiO_2@C nanoparticles anchored on MWNT as high-performance anode materials for Li-ion batteries / Zhao Y., Liu Z., Zhang Y., Mentbayeva A., Wang X., Maximov M.Yu., et al. // Nanoscale Res. Lett. − 2017. − Vol.12. − Art. No. 459.

46. *Carbon-coated* SiO_2 composites as promising anode material for Li-ion batteries / Buga M.R., Spinu-Zaulet A.A., Ungureanu C.G., Mitran R.A., Vasile E., Florea M., et al. // Molecules. − 2021. − Vol.26. − Art. No. 4531.

47. *Hao S., Wang Z., Chen L.* Amorphous SiO_2 in tunnel-structured mesoporous carbon and its anode performance in Li-ion batteries // Mater. Des. − 2016. − Vol.111. − P.616-621.

48. *High* surface area C/SiO_2 composites from rice husks as a high-performance anode for lithium ion batteries / Cui J., Cheng F., Lin J., Yang J., Jiang K., Wen Z., et al. // Powder Technol. − 2017. − Vol.311. − P.1-8.

49. *Synthesis* of SiO_2@carbon-graphene hybrids as anode materials of lithium-ion batteries / Yin L.H., Wu M.B., Li Y.P., Wu G.I., Wang Y.K., Wang Y. // New Carbon Mater. − 2017. − Vol.32. − P.311-318.

50. *Hollow* sandwich-structured N-doped carbon-silica-carbon nanocomposite anode materials for Li ion batteries / Tang X., Zhao C., Li Z., Zhang Y., Gu S. // J. Phys. Conf. Ser. − 2020. − Vol.1520. − Art. No. 012012.

51. *Highly* reversible and fast lithium storage in graphene-wrapped SiO_2 nanotube network / Wang H., Wu P., Qu M., Si L., Tang Y., Zhou Y., et al. // ChemElectroChem. − 2015. − Vol.2. − P.508-511.

52. *Dual-porosity* SiO_2/C nanocomposite with enhanced lithium storage performance / Li H., Wu X., Sun H., Wang K., Fan C., Zhang L., et al. // J. Phys. Chem. C. − 2015. − Vol.119. − P.3495-3501.

53. *Hollow* porous silicon oxide nanobelts for high-performance lithium storage / Wang H., Wu P., Shi H., Tang W., Tang Y., Zhou Y., et al. // J. Power Sources. − 2015. − Vol.274. − P.951-956.

54. *Investigation* of the irreversible reaction mechanism and the reactive trigger on SiO anode material for lithium-ion battery / Yamamura H., Nobuhara K., Nakanishi S., Iba H., Okada S. // J. Ceram. Soc. Jpn. − 2011. − Vol.119. − No. 1395. − P.855-860.

55. *Stress* effect on cycle properties of the silicon thin-film anode / Lee S.J., Lee J.K., Chung S.H., Lee H.Y., Lee S.M., Baik H.K. // J. Power Sources. − 2001. − Vol.97-98. − P.191-193.

56. *Tabuchi T., Yasuda H., Yamachi M.* Li-doping process for Li_xSiO−negative active material synthesized by chemical method for lithium-ion cells // J. Power Sources. − 2005. − Vol.146. − P.507-509.

57. *Seong I.W., Kim K.T., Yoon W.Y.* Electrochemical behavior of a lithium-pre-doped carbon-coated silicon monoxide anode cell // J. Power Sources. − 2008. − Vol.189. − P.511-514.

58. *Metallurgically* lithiated SiO_x anode with high capacity and ambient air compatibility / Zhao J., Lee H.W., Sun J., Yan K., Liu Y., Liu W., et al. // Proc. Natl. Acad. Sci. − 2016. − Vol.113. − P.7408-7413.

59. *Lepoivre F., Larcher D., Tarascon J.M.* Electrochemical activation of silica for enhanced performances of Si-based electrodes // J. Electrochem. Soc. − 2016. − Vol.163. − P.A2791.

60. *Artificial* solid electrolyte interphase-protected Li_xSi nanoparticles: an efficient and stable prelithiation reagent for lithium-ion batteries / Zhao J., Lu Z., Wang H., Liu W., Lee H.W., Yan K., et al. // J. Am. Chem. Soc. − 2015. − Vol.137. − P.8372-8375.

61. *A general* prelithiation approach for group IV elements and corresponding oxides / Zhao J., Sun J., Pei A., Zhou G., Yan K., Liu Y., et al. // Energy Storage Mater. − 2018. − Vol.10. − P.275-281.

62. *Han Y., Liu X., Lu Z.* Systematic investigation of prelithiated SiO_2 particles for high-performance anodes in lithium-ion battery // Appl. Sci. − 2018. − Vol.8. − Art. No. 1245.

63. *Ultrafine* nickel-nanoparticle-enabled SiO_2 hierarchical hollow spheres for high-performance lithium storage / Tang C.J., Liu Y.N., Xu C., Zhu J.X., Wei X.J., Zhou L., et al. // Adv. Funct. Mater. − 2017. − Vol.28. − Art. No. 1704561.

64. *Improvement* of cycle behaviour of SiO/C anode composite by thermochemically generated Li4SiO4 inert phase for lithium batteries / Veluchamy A., Doh C.H., Kim D.H., Lee J.H., Lee D.J., Ha K.H., et al. // J. Power Sources. − 2009. − Vol.188. − P.574-577.

65. *Synergistic* lithium storage in silica−tin composites enables a cycle-stable and high-capacity anode for lithium-ion batteries / Ding X., Liang D., Ai X., Zhao H., Zhang N., Chen X., et al. // ACS Appl. Energy Mater. − 2021. − Vol.4. − P.2741-2750.

66. *Lee S.S., Park C.M.* Amorphous silicon dioxide-based composites for high-performance Li-ion battery anodes //

Electrochim. Acta. − 2018. − Vol.284. − P.220-225.

67. *Metal-organic* framework@SiO₂ as permselective separator for lithium-sulfur batteries / Suriyakumar S., Stephan A.M., Angulakshmi N., Hassan M.H., Alkordi M.H. // J. Mater. Chem. A. − 2018. − Vol.6. − P.14623-14632.

ПРО ШЛЯХИ ПЕРЕТВОРЕННЯ ДІОКСИДУ КРЕМНІЮ SIO₂ В ЛІТІЄВИХ АКУМУЛЯТОРНИХ СИСТЕМАХ: ОГЛЯД

Апостолова Р.Д., Шембель О.М.

Сполуки кремнію та оксиду кремнію SiO, SiO₂, SiOₓ та SiOC розглядаються як перспективне сімейство матеріалів для високоенергетичних літієвих батарей завдяки високій теоретичній ємності, широкому поширенню в природі, низькій вартості, екологічній безпеці та простоті синтезу. Сполуки оксиду кремнію замінили кремній в надії покращити характеристики розряду літієвих батарей. Оксиди кремнію демонструють чудову стабільність під час циклювання після оптимізації структури. Однак вони страждають від проблеми низької кулонівської ефективності та високого гістерезису напруги (різниці в напрузі заряду та розряду), що перешкоджає їх практичному застосуванню. Значне об'ємне розширення оксидів кремнію під час циклювання та необоротна втрата ємності на початкових циклах є перешкодою для їх широкомасштабного практичного використання. У цьому огляді розглядаються особливості перетворення SiO₂ та його гібридних сполук в окисно-відновній реакції з літієм та шляхи подолання існуючих проблем. Діоксид кремнію більш стійкий до об'ємного розширення, ніж кремній. Для літієвих батарей були розроблені та випробувані різні структурні формати нанометрового SiO₂, такі як нанотрубки, наностржні, нанодроти, наночастинки, тонкі плівки. Для вирішення проблем у системі SiO₂/Li також запропоновано та досліджено низку композитів SiO₂ з вуглецем, графеном, активними та неактивними металами тощо. Аналізуючи результати досліджень, встановлено значну роль міжфазної плівки твердого електроліту в ефективній конверсії SiO₂. У свою чергу, утворення плівки на діоксиді кремнію залежить від методу синтезу діоксиду, який вносить домішки в кінцевий продукт синтезу. Домішки сприяють спотворенню міжфазної плівки твердого електроліту під час циклу системи SiO₂/Li та втраті розрядної ємності. Діоксид SiO₂, одержаний у сухому середовищі кульового млина, вигідно відрізняється від одержаного з розчинів. Було докладено багато зусиль, щоб подолати проблеми електродних матеріалів, що містять Si, однак вони повинні пройти певний шлях для широкомасштабного практичного застосування.

ON WAYS OF CONVERSION OF SILICON DIOXIDE SiO₂ IN LITHIUM BATTERY SYSTEMS: A REVIEW

R.D. Apostolova *, E.M. Shembel

Ukrainian State University of Chemical Technology, Dnipro, Ukraine

* e-mail: apostolova.rd@gmail.com

Silicon and silicon oxide compounds SiO, SiO₂, SiOₓ and SiOC are considered as a promising family of materials for high-energy lithium batteries due to their high theoretical capacity, widespread in nature, low cost, environmental safety and ease of synthesis. Silicon oxide compounds have replaced silicon in the hope of improving the discharge characteristics of lithium batteries. Oxides of silicon show excellent stability during cycling after structure optimization. However, they suffer from the problem of low Coulomb efficiency and high voltage hysteresis (difference in charge and discharge voltage), which prevents their practical application. Significant bulk expansion of silicon oxides during cycling and irreversible loss of capacity in the initial cycles are an obstacle to their large-scale practical use. This review pays attention to the peculiarities of the conversion of SiO₂ and its hybrid compounds into the redox reaction with lithium and ways to overcome existing problems. Silicon dioxide is more resistant to bulk expansion than silicon. Various structural formats of nanometer SiO₂ have been developed and tested for lithium batteries, such as nanotubes, nanorods, nanowires, nanoparticles, thin films. To solve problems in the SiO₂/Li system, a number of SiO₂ composites with carbon, graphene, active and inactive metals, etc. have also been proposed and studied. Analyzing the results of the studies, we found a significant role of the solid electrolyte interphase film in the efficient conversion of SiO₂. In turn, the formation of a film on silicon dioxide depends on the method of synthesis of dioxide, which introduces impurities into the final synthesis product. Impurities contribute to the distortion of the solid electrolyte interphase film during the cycling of the SiO₂/Li system, and the loss of discharge capacity. SiO₂ dioxide obtained in a dry environment of a ball mill differs favorably from that obtained from solutions. Many efforts have been made to overcome the problems in Si-containing electrode materials, however, they have to go a certain way for large-scale practical application.

Keywords: silicon oxide; silicon; lithium-ion battery; electrochemical transformation pathway; degradation process; composite compound; problem-solving strategy.

REFERENCES

1. Huang H, Kelder EM, Chen L, Schoonman J. Electrochemical characteristics of Sn₁₋ₓSiₓO₂ as anode for lithium-ion batteries. *J Power Sources*. 1999; 81-82: 362-367. doi: 10.1016/S0378-7753(98)00219-5.

2. Saint J, Moncrette M, Larcher D, Laffont L, Beattie S, Peres JP, et al. Towards a fundamental understanding of the improved electrochemical performance of silicon-carbon composites. *Adv Funct Mater*. 2007; 17: 1765-1774. doi: 10.1002/adfm.200600937.

3. Obrovac MN, Christensen L. Structural changes in silicon anodes during lithium insertion/extraction. *Electrochem Solid-State Lett*. 2004; 7: A93. doi: 10.1149/1.1652421.

4. Liu Z, Yu Q, Zhao Y, He R, Xu M, Feng S, et al. Silicon oxides: a promising family of anode materials for lithium-ion batteries. *Chem Soc Rev*. 2019; 48: 285-309. doi: 10.1039/C8CS00441B.

5. Apostolova RD, Zaderey ND, Kirsanova IV. Reshenie problem povysheniya energoemkosti i stabilnosti tsiklirovaniya Si-, SiO-, SiO_2-electrodov dlya litiy-ionnykh istochnikov toka: analiticheskiy obzor [The ways of increasing the power intensity and stable cycling of Si-, SiO-, SiO_2-electrodes in lithium-ion power sources: a review]. *Voprosy Khimii i Khimicheskoi Tekhnologii*. 2016; (5-6): 31-52. (*in Russian*).

6. Ban C, Kappes BB, Xu Q, Engtrakul C, Ciobanu CV, Dillon AC, et al. Lithiation of silica through partial reduction. *Appl Phys Lett*. 2012; 100: 243905. doi: 10.1063/1.4729743.

7. Zhang Y, Li Y, Wang Z, Zhao K. Lithiation of SiO_2 in Li-ion batteries: in situ transmission electron microscopy experiments and theoretical studies. *Nano Lett*. 2014; 14: 7161-7170. doi: 10.1021/nl503776u.

8. Perez-Beltran S, Ramirez-Caballero GE, Balbuena PB. First-principles calculations of lithiation of a hydroxylated surface of amorphous silicon dioxide. *J Phys Chem C*. 2015; 119: 16424-16431. doi: 10.1021/acs.jpcc.5b02992.

9. Ostadhossein A, Kim SY, Cubuk ED, Qi Y, van Duin ACT. Atomic insight into the lithium storage and diffusion mechanism of SiO_2/Al_2O_3 electrodes of lithium ion batteries: Reax FF reactive force field modeling. *J Phys Chem A*. 2016; 120: 2114-2127. doi: 10.1021/acs.jpca.5b11908.

10. Lener G, Otero M, Barraco DE, Leiva EPM. Energetics of silica lithiation and its applications to lithium ion batteries. *Electrochim Acta*. 2018; 259: 1053-1058. doi: 10.1016/j.electacta.2017.10.126.

11. Guo B, Shu J, Wang Z, Yang H, Shi L, Liu Y, et al. Electrochemical reduction of nano-SiO_2 in hard carbon as anode material for lithium ion batteries. *Electrochem Commun*. 2008; 10: 1876-1878. doi: 10.1016/j.elecom.2008.09.032.

12. Graetz J, Ahn CC, Yazami R, Fultz Z. Highly reversible lithium storage in nanostructured silicon. *Electrochem Solid-State Lett*. 2003; 6: A194. doi: 10.1149/1.1596917.

13. Mironjuk IF, Ogenko VM, Ostafejchuk BK, Mandzjuk VI, Grigorchuk II. Termodinamichni osoblyvosti strumoutvoruyuchogo protsesu v litiyevykh dzherelakh strumu z katodom na osnovi pirogennogo dioksydu kremniyu [Thermodynamic features of the current-forming process in lithium sources with a cathode based on pyrogenic silicon dioxide]. *Fizika i Khimiya Tverdogo Tila*. 2001; 2: 661. (*in Ukrainian*).

14. Chang WS, Park CM, Kim JH, Kim YU, Jeong G, Sohn HJ. Quartz (SiO_2): a new energy storage anode material for Li-ion batteries. *Energy Environ Sci*. 2012; 5: 6895-6899. doi: 10.1039/C2EE00003B.

15. Guo YG, Hu JS, Wan LJ. Nanostructured materials for electrochemical energy conversion and storage devices. *Adv Mater*. 2008; 20: 2878-2887. doi: 10.1002/adma.200800627.

16. Bruce PG, Scrosati B, Tarascon JM. Nanomaterials for rechargeable lithium batteries. *Angew Chem Int Ed*. 2008; 47: 2930-2946. doi: 10.1002/anie.200702505.

17. Dong X, Zheng X, Deng Y, Wang L, Hong H, Ju Z. SiO_2/N-doped graphene aerogel composite anode for lithium-ion batteries. *J Mater Sci*. 2020; 55: 13023-13035. doi: 10.1007/s10853-020-04905-y.

18. Sun Y, Liu N, Cui Y. Promises and challenges of nanomaterials for lithium-based rechargeable batteries. *Nat Energy*. 2016; 1: 16071. doi: 10.1038/nenergy.2016.71.

19. Yan D, Geng X, Zhao Y, Lin X, Liu X. Phase relations of $Li_2O-FeO-SiO_2$ ternary system and electrochemical properties of $Li_xSi_yO_z$ compounds. *J Mater Sci*. 2016; 51: 6452-6463. doi: 10.1007/s10853-016-9943-2.

20. Ratynski M, Hamankiewicz B, Buchberger AD, Czerwinski A. Surface oxidation of nano-silicon as a method for cycle life enhancement of Li-ion active materials. *Molecules*. 2020; 25: 4093. doi: 10.3390/molecules25184093.

21. Schnabel M, Arca E, Ha Y, Stetson C, Teeter G, Han SD, et al. Enhanced interfacial stability of Si anodes for Li-ion batteries via surface SiO_2 coating. *ACS Appl Energy Mater*. 2020; 3: 8842-8849. doi: 10.1021/acsaem.0c01337.

22. Xun S, Song X, Wang L, Grass ME, Liu Z, Battaglia VS, et al. The effects of native oxides surface layer on the electrochemical performance of Si nanoparticle-based electrodes. *J Electrochem Soc*. 2011; 158: A1260. doi: 10.1149/2.007112jes.

23. Moon J, Park MS, Cho M. Anisotropic compositional expansion and chemical potential of lithiated SiO_2 electrodes: multiscale mechanical analysis. *ACS Appl Mater Interfaces*. 2019; 11: 19183-19190. doi: 10.1021/acsami.9b04352.

24. Apostolova RD, Matsievskii NA, Gladun VA, Savchenko MO. Thin-layer electrochemically produced SiO_2/Ni composites in a prototyping lithium-ion battery. *Surf Eng Appl Electrochem*. 2018; 54: 420-426. doi: 10.3103/S1068375518040026.

25. Apostolova RD, Nagirnyi VM, Shembel EM. Razrabotka i issledovaniye katodnogo materiala $LiCoO_2$ na osnove electroliticheskogo oksida kobalta [Development and research of cathode material $LiCoO_2$ based on electrolytic cobalt oxide]. *Russ J Electrochem*. 1998; 34: 778. (*in Russian*).

26. Astrova EV, Fjedulova GV, Smirnova IA, Remenjuk AD, Kulova TL, Skundin AM. Otritsatelnye elektrody dlya litii-ionnykh akumulatorov na osnove poristogo kremniya [Negative electrodes for lithium-ion batteries based on porous silicon]. *Pisma v Zhurnal Tekhnicheskoi Fiziki*. 2011; 37: 87.

27. Sun Q, Zhang B, Fu ZW. Lithium electrochemistry of SiO_2 thin film electrode for lithium-ion batteries. *Appl Surf Sci*. 2008; 254: 3774-3779. doi: 10.1016/j.apsusc.2007.11.058.

28. Limthongkul P, Jang YI, Dudeny NJ, Chiang YM. Electrochemically-driven solid-state amorphization in lithium-silicon alloys and implications for lithium storage. *Acta Mater*. 2003; 51: 1103-1113. doi: 10.1016/s1359-6454(02)00514-1.

29. Yang J, Takeda Y, Imanishi N, Capiglia C, Xie JY, Yamamoto O. SiO_x-based anodes for secondary lithium batteries. *Solid State Ionics*. 2002; 152-153: 125-129. doi: 10.1016/s0167-2738(02)00362-4.

30. Miyachi M, Yamamoto H, Kawai H, Ohta T, Shirakata M. Analysis of SiO anodes for lithium-ion batteries. *J Electrochem Soc.* 2005; 152: A2089-A2091. doi: 10.1149/1.2013210.

31. Li X, Dhanabalan A, Meng X, Gu L, Sun X, Wang C. Nanoporous tree-like SiO_2 films fabricated by sol-gel assisted electrostatic spray deposition. *Microporous Mesoporous Mater.* 2012; 151: 488-494. doi: 10.1016/j.micromeso.2011.09.003.

32. Yao Y, Zhang J, Xue L, Huang T, Yu A. Carbon-coated SiO_2 nanoparticles as anode material for lithium ion batteries. *J Power Sources.* 2011; 196: 10240-10243. doi: 10.1016/j.jpowsour.2011.08.009.

33. Yang Y, Gao Y, Liu J, Fang X. Hydrothermal synthesis and electrochemical performance of amorphous SiO_2 nanospheres/ graphene composites. *Mater Sci Appl.* 2017; 8: 959-965. doi: 10.4236/msa.2017.813070.

34. Favors Z, Wang W, Bay HH, George A, Ozkan M, Ozkan CS. Stable cycling of SiO_2 nanotubes as high-performance anodes for lithium-ion batteries. *Sci Rep.* 2014; 4: 4605. doi: 10.1038/srep04605.

35. Liang J, Yang S, Ye L, Li X, Yang X, Chen S, et al. In situ synthesis of silica/graphite anode material with enhanced lithium storage performance. *J Mater Sci Mater Electron.* 2021; 32: 28119-28128. doi: 10.1007/s10854-021-07187-5.

36. Yan N, Wang F, Zhong H, Li Y, Wang Y, Hu L, et al. Hollow porous SiO_2 nanocubes towards high-performance anodes for lithium-ion batteries. *Sci Rep.* 2013; 3: 1568. doi: 10.1038/srep01568.

37. Yao Y, Zhang J, Xue L, Huang T, Yu A. Carbon-coated SiO_2 nanoparticles as anode material for lithium ion batteries. *J Power Sources.* 2011; 196: 10240-10243. doi: 10.1016/j.jpowsour.2011.08.009.

38. Li W, Wang F, Ma M, Zhou J, Liu Y, Chen Y. Preparation of SiO_2 nanowire arrays as anode material with enhanced lithium storage performance. *RSC Adv.* 2018; 8: 33652-33658. doi: 10.1039/C8RA06381H.

39. Sivonxay E, Aykol M, Persson KA. The lithiation process and Li diffusion in amorphous SiO_2 and Si from first-principles. *Electrochim Acta.* 2020; 331: 135344. doi: 10.1016/j.electacta.2019.135344.

40. Sasidharan M, Liu D, Gunawardhana N, Yoshio M, Nakashima K. Synthesis, characterization and application for lithium-ion rechargeable batteries of hollow silica nanospheres. *J Mater Chem.* 2011; 21: 13881-13888. doi: 10.1039/c1jm10864f.

41. Yang X, Huang H, Li Z, Zhong M, Zhang G, Wu D. Preparation and lithium-storage performance of carbon/silica composite with a unique porous bicontinuous nanostructure. *Carbon.* 2014; 77: 275-280. doi: 10.1016/j.carbon.2014.05.030.

42. Arumugam D, Kalaignan GP. Synthesis and electrochemical characterizations of nano-SiO_2-coated $LiMn_2O_4$ cathode materials for rechargeable lithium batteries. *J Electroanal Chem.* 2008; 624: 197-204. doi: 10.1016/j.jelechem.2008.09.007.

43. Yu Y, Shui JL, Jin Y, Chen CH. Electrochemical performance of nano-SiO_2 modified $LiCoO_2$ thin films fabricated by electrostatic spray deposition (ESD). *Electrochim Acta.* 2006; 51: 3292-3296. doi: 10.1016/j.electacta.2005.09.021.

44. Matzijevskiy NA, Apostolova RD, Savchenko MO, Gladun A. Improvement of FeS characteristics in Li accumulators by electrochemical codeposition with SiO_2. In: Barsukov VZ, editor. *Promising materials and processes in technical electrochemistry.* Kyiv: KNUTD Publishers; 2016. p. 68-73.

45. Zhao Y, Liu Z, Zhang Y, Mentbayeva A, Wang X, Maximov MYu, et al. Facile synthesis of SiO_2@C nanoparticles anchored on MWNT as high-performance anode materials for Li-ion batteries. *Nanoscale Res Lett.* 2017; 12: 459. doi: 10.1186/s11671-017-2276-2.

46. Buga MR, Spinu-Zaulet AA, Ungureanu CG, Mitran RA, Vasile E, Florea M, et al. Carbon-coated SiO_2 composites as promising anode material for Li-ion batteries. *Molecules.* 2021; 26: 4531. doi: 10.3390/molecules26154531.

47. Hao S, Wang Z, Chen L. Amorphous SiO_2 in tunnel-structured mesoporous carbon and its anode performance in Li-ion batteries. *Mater Des.* 2016; 111: 616-621. doi: 10.1016/j.matdes.2016.09.020.

48. Cui J, Cheng F, Lin J, Yang J, Jiang K, Wen Z, et al. High surface area C/SiO_2 composites from rice husks as a high-performance anode for lithium ion batteries. *Powder Technol.* 2017; 311: 1-8. doi: 10.1016/j.powtec.2017.01.083.

49. Yin LH, Wu MB, Li YP, Wu GI, Wang YK, Wang Y. Synthesis of SiO_2@carbon-graphene hybrids as anode materials of lithium-ion batteries. *New Carbon Mater.* 2017; 32: 311-318. doi: 10.1016/S1872-5805(17)60124-0.

50. Tang X, Zhao C, Li Z, Zhang Y, Gu S. Hollow sandwich-structured N-doped carbon-silica-carbon nanocomposite anode materials for Li ion batteries. *J Phys Conf Ser.* 2020; 1520: 012012. doi: 10.1088/1742-6596/1520/1/012012.

51. Wang H, Wu P, Qu M, Si L, Tang Y, Zhou Y, et al. Highly reversible and fast lithium storage in graphene-wrapped SiO_2 nanotube network. *ChemElectroChem.* 2015; 2: 508-511. doi: 10.1002/celc.201402370.

52. Li H, Wu X, Sun H, Wang K, Fan C, Zhang L, et al. Dual-porosity SiO_2/C nanocomposite with enhanced lithium storage performance. *J Phys Chem C.* 2015; 119: 3495-3501. doi: 10.1021/jp511435w.

53. Wang H, Wu P, Shi H, Tang W, Tang Y, Zhou Y, et al. Hollow porous silicon oxide nanobelts for high-performance lithium storage. *J Power Sources.* 2015; 274: 951-956. doi: 10.1016/j.jpowsour.2014.10.180.

54. Yamamura H, Nobuhara K, Nakanishi S, Iba H, Okada S. Investigation of the irreversible reaction mechanism and the reactive trigger on SiO anode material for lithium-ion battery. *J Ceram Soc Jpn.* 2011; 119(1395): 855-860. doi: 10.2109/jcersj2.119.763.

55. Lee SJ, Lee JK, Chung SH, Lee HY, Lee SM, Baik HK. Stress effect on cycle properties of the silicon thin-film anode. *J Power Sources.* 2001; 97-98: 191-193. doi: 10.1016/S0378-7753(01)00761-3.

56. Tabuchi T, Yasuda H, Yamachi M. Li-doping process for Li_xSiO−negative active material synthesized by chemical method for lithium-ion cells. *J Power Sources.* 2005; 146: 507-509. doi: 10.1016/j.jpowsour.2005.03.100.

57. Seong IW, Kim KT, Yoon WY. Electrochemical behavior of a lithium-pre-doped carbon-coated silicon monoxide anode cell. *J Power Sources*. 2008; 189: 511-514. doi: 10.1016/j.jpowsour.2008.11.029.

58. Zhao J, Lee HW, Sun J, Yan K, Liu Y, Liu W, et al. Metallurgically lithiated SiO_x anode with high capacity and ambient air compatibility. *Proc Natl Acad Sci*. 2016; 113: 7408-7413. doi: 10.1073/pnas.1603810113.

59. Lepoivre F, Larcher D, Tarascon JM. Electrochemical activation of silica for enhanced performances of Si-based electrodes. *J Electrochem Soc*. 2016; 163: A2791. doi: 10.1149/2.1221613jes.

60. Zhao J, Lu Z, Wang H, Liu W, Lee HW, Yan K, et al. Artificial solid electrolyte interphase-protected Li_xSi nanoparticles: an efficient and stable prelithiation reagent for lithium-ion batteries. *J Am Chem Soc*. 2015; 137: 8372-8375. doi: 10.1021/jacs.5b04526.

61. Zhao J, Sun J, Pei A, Zhou G, Yan K, Liu Y, et al. A general prelithiation approach for group IV elements and corresponding oxides. *Energy Storage Mater*. 2018; 10: 275-281. doi: 10.1016/j.ensm.2017.06.013.

62. Han Y, Liu X, Lu Z. Systematic investigation of prelithiated SiO_2 particles for high-performance anodes in lithium-ion battery. *Appl Sci*. 2018; 8: 1245. doi: 10.3390/app8081245.

63. Tang CJ, Liu YN, Xu C, Zhu JX, Wei XJ, Zhou L, et al. Ultrafine nickel-nanoparticle-enabled SiO_2 hierarchical hollow spheres for high-performance lithium storage. *Adv Funct Mater*. 2017; 28: 1704561. doi: 10.1002/adfm.201704561.

64. Veluchamy A, Doh CH, Kim DH, Lee JH, Lee DJ, Ha KH, et al. Improvement of cycle behaviour of SiO/C anode composite by thermochemically generated Li_4SiO_4 inert phase for lithium batteries. *J Power Sources*. 2009; 188: 574-577. doi: 10.1016/j.jpowsour.2008.11.137.

65. Ding X, Liang D, Ai X, Zhao H, Zhang N, Chen X, et al. Synergistic lithium storage in silica−tin composites enables a cycle-stable and high-capacity anode for lithium-ion batteries. *ACS Appl Energy Mater*. 2021; 4: 2741-2750. doi: 10.1021/acsaem.1c00023.

66. Lee SS, Park CM. Amorphous silicon dioxide-based composites for high-performance Li-ion battery anodes. *Electrochim Acta*. 2018; 284: 220-225. doi: 10.1016/j.electacta.2018.07.160.

67. Suriyakumar S, Stephan AM, Angulakshmi N, Hassan MH, Alkordi MH. Metal-organic framework@SiO_2 as permselective separator for lithium-sulfur batteries. *J Mater Chem A*. 2018; 6: 14623-14632. doi: 10.1039/C8TA02259C.